2023

ADSORPTION OF CADMIUM AND LEAD IONS USING BIOWASTE ADSORBENTS FROM AQUEOUS SOLUTIONS WITH ION-SELECTIVE ELECTRODES AND ICP-OES

Taha Fadlou Allah

ADSORPTION OF CADMIUM AND LEAD IONS USING BIOWASTE ADSORBENTS FROM AQUEOUS SOLUTIONS WITH ION-SELECTIVE ELECTRODES AND ICP-OES

A thesis submitted in partial fulfillment
of the requirements for the degree of

MASTER OF SCIENCE

to the faculty of the

DEPARTMENT OF CHEMISTRY

of

ST. JOHN'S COLLEGE OF LIBERAL ARTS AND SCIENCES

at

ST. JOHN'S UNIVERSITY
New York
by
TAHA FADLOU ALLAH

Date Submitted: _____ Date Approved: _____

_____ _____

Taha Fadlou Allah Enju Wang, Ph. D

ABSTRACT

ADSORPTION OF CADMIUM AND LEAD IONS USING BIOWASTE ADSORBENTS FROM AQUEOUS SOLUTIONS WITH ION-SELECTIVE ELECTRODES AND ICP-OES

Taha Fadlou Allah

Upon using low cost biowaste adsorbents as toxic metal ion removal substrates from aqueous solutions, it was found that they have a high potential of being used to generate a great environmental advantage. This thesis study evaluated pumpkin peels and potato peels for the adsorption of cadmium and lead ions. Chamomile tea residues, peanut shells, and ground coffee beans were also studied and showed less adsorption response for these heavy metals. The biowaste sorbents were treated with acid (HNO_3) or base (NaOH). Batch experiments were carried by introducing a known concentration of metal ion solution into the biowaste sorbent at various pH levels. The pH and metal ions were monitored with a pH and cadmium or lead ion-selective electrode continuously for two hours, and the final concentration for the metal ions after 24 hours was measured with the ISE and then confirmed with ICP-OES. The characteristics of the biowaste sorbents were also studied with scanning electron microscope (SEM) and infrared spectra (FTIR). L-type isotherms were obtained that fit to Freundlich model. Adsorption isotherms showed chemical adsorption and kinetics following second order model. Equilibrium adsorption capacity is higher than 55 mg/g for both ions at pH 5.6 when the initial concentration is 500 ppm. Dynamic cadmium adsorption capacity is 12-15 mg/g from aqueous solution when the feed solution is 220 ppm. The biowaste materials can also be regenerated with acid washing. This work demonstrates that the ion-selective electrodes can provide

simple and fast continuous determination of metal ion concentrations during the adsorption process.

ACKNOWLEDGEMENTS

I would like to express my immense gratitude and profound regard to my mentor and advisor, Dr. Enju Wang, for her help with the research and in compiling this thesis. Her guidance and valuable feedback have been extremely helpful throughout my journey and accomplishments.

I would also like to thank Dr. Anne Vazquez and Dr. Tianchan Jiang for agreeing and taking the time to be part of my thesis committee. Their contributions and comments have been invaluable, and I am grateful that they have been able to join me in my journey.

I am and will always be grateful to my family. My father Islam Fadlou Allah, my mother Khadija Bouhnas, my sister Malak Fadlou-Allah, and my brother Mohamed Yahya Fadlou Allah, have all been very supportive in my life and my love for them goes beyond any words.

I would also like to express my gratitude to Dr. Joseph Serafin and the entire staff of the St. John's Chemistry Department for allowing me to be a part of this extraordinary journey. Without the department's support, my research would not have been possible.

TABLE OF CONTENTS

ACKNOWLEDGEMENTS ……..……..…..ii
LIST OF TABLES……...v
LIST OF FIGURES ……..……..vi
CHAPTER 1: INTRODUCTION……1
1.1. WATER POLLUTION FROM CADMIUM AND LEAD ……..……1
1.2. ADSORPTION .....……..……3
1.2.1. Biowaste Sorbents……...…….……...…….3
1.2.1.1. Potato peels ……3
1.2.1.2. Pumpkin peels……4
1.2.2. Adsorption Theory……...5
1.2.2.1. Langmuir Adsorption Isotherm ……..6
1.2.2.2. Freundlich Adsorption Isotherm……6
1.3. ION-SELECTIVE ELECTRODES ...……...7
1.3.1. pH Electrodes……...8
1.3.2. Cadmium and Lead Ion Selective Electrodes …..……9
1.4. INDUCTIVELY COUPLED PLASMA OPTICAL EMISSION SPECTROSCOPY……..12
1.5. INFRARED SPECTROSCOPY ……14
1.6. SCANNING ELECTRON MICROSCOPY ……...15
1.7. CURRENT RESEARCH AND OBJECTIVES……..16
CHAPTER 2: MATERIALS AND METHODS……18
2.1. CHEMICALS AND REAGENTS ……..……..……..18
2.1.1. Metal Ion Solutions……18
2.1.2. Buffer Solutions ……18
2.2. INSTRUMENTATION ……..19
2.2.1. Ion-Selective Electrodes ……19
2.2.2. FTIR……...20
2.2.3. ICP-OES ……20
2.3. BIOWASTE SORBENTS ……..20
2.4. BATCH EXPERIMENTS ……..21
2.5. ADSORPTION KINETICS……22
2.6. DYNAMIC ADSORPTION AND DESORPTION/RECOVERY OF THE BIOSORBENTS ……..23
CHAPTER 3: RESULTS AND DISCUSSION……24
3.1. CALIBRATION CURVES……..……24
3.2. PRELIMINARY RESULTS……26
3.3. BIOSORBENT CHARACTERIZATION……27
3.3.1. FTIR ……27
3.3.2. Sorbent Morphology……29
3.4. CADMIUM ADSORPTION ……30
3.4.1. Time response monitored with Cadmium ISE ……30
3.4.2. Cadmium Adsorption Isotherms ……34
3.4.3. Column Adsorption of Cadmium……38

3.5. LEAD ADSORPTION ……40
3.5.1. Time response monitored with Lead ISE ……40
3.5.2. Lead Adsorption Isotherms ……41
CHAPTER 4: CONCLUSION ……..44
REFERENCES ……..45

LIST OF TABLES

Table 1. Calibration statistics for ICP-OES and ion-selective electrodes ……25

Table 2. Sorbent Screening using Cd (II)-ISE with 220 ppm Cd (II) solutions over 2 hours for various biosorbents…….26

Table 3. Freundlich isotherm fitting and kinetics constants for 440 ppm of Cd (II) at various sorbents measured with Cd (II)-ISE …….34

Table 4. Freundlich isotherm fitting and kinetics constants for Pb (II) ion at various sorbents measured with Pb (II)-ISE and ICP at a pH of 5.6 with 250 ppm initial Pb (II) concentration……..42

LIST OF FIGURES

Figure 1. Biosorbent mechanisms ……...5

Figure 2. Schematic Diagram of an Ion-Selective Electrode……..7

Figure 3. Structure of a Pb (II) or Cd (II) ISE…….9

Figure 4. Electrode Potential vs Solution pH in Cadmium Ion Solutions at 25 °C ……..11

Figure 5. Electrode Potential vs Solution pH in Lead Ion Solutions at 25 °C ……..12

Figure 6. FTIR spectrum of D-glucose ……15

Figure 7. Calibration curves for (a) Cd and (b) Pb with ICP-OES in 2% nitric acid……24

Figure 8. Calibration curves for (a) Cd (II) and (b) Pb (II) ion-selective electrodes in acetic acid buffer, pH 5.6 ……...25

Figure 9. FTIR spectra of base treated pumpkin peel before and after Pb (II) Adsorption ……27

Figure 10. FTIR spectra of base treated pumpkin peel before and after Cd (II) Adsorption ……28

Figure 11. Scanning electron microscopy of (a) pumpkin peel and (b) potato peel porous biosorbents ……29

Figure 12. (a) Time response of the Cd((II)-ISE with 20 mL of 440 ppm initial cadmium in water when 0.10 g of base treated pumpkin peel was added. (b), Linear plot of the second order model ……31

Figure 13. (a) Time response of the Cd((II)-ISE with 20 mL of (▪)440 ppm, (●) 220 ppm initial cadmium in acetate buffer pH 5.6 when 0.10 g of base treated pumpkin peel was added. (b), Linear plot of the second order model ……32

Figure 14. (a) Time response of the Cd((II)-ISE with 20 mL of (▪)440 ppm, (●) 220 ppm initial cadmium in acetate buffer pH 5.6 when 0.10 g of base treated potato peel was added. (b), Linear plot of the second order model ……33

Figure 15. Variation of pH along the adsorption reaction of Cd (II) at various initial Cd(II) concentrations with base treated substrates (▪) potato peel, (●) pumpkin peel …..35

Figure 16. (a) Adsorption isotherm and (b) Freundlich fitting equations for Cd (II) adsorption on base treated (▪) potato and (●) pumpkin peel biosorbents ……..37

Figure 17. Adsorption isotherms and Freundlich fitting equations for Cd (II) adsorption on base treated potato sorbents using equilibrium concentrations measured with ICP and ISE ……38

Figure 18. Column Cd^{2+} adsorption with 200 ppm Cd^{2+} in dilute pH 7.2 Tris-HCl buffer as feeding solution. (a) Cd (II)-ISE potential (b) pH vs. the solution volume Collected ……39

Figure 19. (a) Time response of the lead (II) electrode with 40 mL of 500 ppm initial lead concentration in acetic acid buffer of pH 5.6 when 0.20 g of base treated potato peel was added. (b) Linear plot of the second order model ……..40

Figure 20. (a) Adsorption isotherm and (b) Freundlich fitting equations for Pb (II) adsorption on base treated potato biosorbents ……..41

Figure 21. Adsorption mechanism of carboxylic acid groups containing adsorbent polymer for lead ion ……43

CHAPTER 1:

INTRODUCTION

1.1. WATER POLLUTION FROM CADMIUM AND LEAD

Ever since the 18th century, the environment has become increasingly more exposed to pollutants that threaten the safety of its inhabitants. The hasty development of industrialization not only impacted the quality of air, but also drastically diminished the quality of drinking water. Over the last few decades, pollution of water has been a high concern from both natural and anthropogenic sources.

Another apprehensive fact of pollution is the high presence of contaminants in the environment, especially those with toxic and hazardous properties [1-2]. Some of the major contaminants that affect the safety of drinking water are the presence of heavy metals at a concentration higher than the permissible standard [1]. The metals that pose the most risk to humans include cadmium, lead, arsenic, mercury, zinc, copper, chromium, and nickel.

Over exposure to these metals may lead to severe cases of illness and often death. Cadmium toxicity and lead poisoning pose detrimental effects to the human body upon overexposure to these metals. The most significant natural sources of cadmium pollution in water are the weathering of rocks leading to cadmium release into soils and waterways, and airborne soil particles from forest fires and volcanic activity. There are also anthropogenic sources of cadmium emission resulting from non-ferrous metal production, stationary fossil fuel combustion, and iron and steel production [3].

Lead pollution in water has been a major problem in the past and there have been many regulations imposed over the past few decades to reduce lead usage and water

contamination. However, many areas still have major exposure to lead in drinking water, especially third world countries where no such regulations are imposed [4]. Like cadmium pollution, some natural sources of lead pollution include forest fires and volcanic activities. In addition, because lead is a naturally occurring element, erosion of natural deposits of lead as well as leaching from lead-containing minerals can lead to water contamination [5]. There are also anthropogenic sources that lead to water contamination. One of the most common sources is from the corrosion of plumbing materials in lead pipes [6]. Other sources that contribute to lead pollution include manufacturing and disposing or lead batteries, leaded gasoline and aviation fuel, and other electronic equipment that are not properly disposed [7].

Cadmium affects the human body at a cellular level. At high concentrations, cadmium is carcinogenic and can interact with DNA repair mechanisms and may even lead to the generation of reactive oxygen species. Even at lower concentrations, cadmium interacts with the mitochondria and inhibits many cellular respiration processes [2]. At a non-cellular level, cadmium toxicity negatively affects the renal, reproductive, and cardiovascular systems. Similarly, lead poisoning can have even more adverse effects on the human body. Lead can easily be absorbed through the circulatory system and directly affects major organ systems such as nervous, cardiovascular, renal, and immune systems [3]. In addition to lead also being carcinogenic, exposure at high concentrations has been known to cause permanent damage to the brain and can often lead to death. [8].

1.2. ADSORPTION

1.2.1. Biowaste Sorbents

With a high amount of contaminants, remediation of the environment has an enormous cost, and reducing pollution is critical. The big challenge currently is to find the most eco-friendly path that leads to the decontamination of the environment. One potential solution to remove these contaminants from drinking water is the use of low cost biowaste adsorbents [9-19]. The biowaste adsorbent surfaces are known to have COOH, C=O, C=C, CONH, NH and OCH functional groups that could physically adsorb, ion-exchange or chemically complex with metal ions, thus retaining them especially when these groups are above the iso-electric point. The most prominent chemical feature of bio sorbents that make it effective for adsorbing metal ions is the presence of several kinds of polysaccharides including pectic acid, alginic acid, and chitosan. Polyphenol compounds and other proteins present in bio sorbents may also aid in the adsorption process of metal ions. Although some sorbents may not exhibit significant adsorption activity naturally, it has been shown that treatment of sorbents, such as using sodium hydroxide, may significantly improve the adsorption process [20]. While there is a lot of work done with various biowaste sorbents, there is less work done with the pumpkin and potato peels for cadmium and lead adsorption. The major advantages of using pumpkin and potato peels are their low costs and high availability within the environment.

1.2.1.1. Potato peels.

Potatoes, known scientifically as Solanum Tuberlosum L., are one of the most widely consumed vegetables in the world. Potatoes are rich in nutrients and are highly versatile in their application. Because of its high demand in the market, global production

of potatoes has reached approximately 368 million tons in 2018 [21]. Despite containing a significant amount of the potato's nutritional value, potato peels are often discarded and remain unused. Although the specific reason is unclear, it maybe be suspected by a few that the peel of a potato may be more exposed to other chemicals and pesticides if they are not grown organically.

The chemical composition of potato peels is predominated by carbohydrates when water is excluded as a factor. A study showed that potato peels contained 25% starch, 30% non-starch polysaccharides, 18% proteins, 20% acid-soluble and acid-insoluble lignin, 1% lipids, and 6% ash [22]. There are also various phenolic acids present in potato peels, such as gallic acid, protocatechuic acid, vanillic acid, caffeic acid, chlorogenic acid, p-hydroxybenzoic acid and p-coumaric acid [22]. These phenolic acids are hypothesized to play an important role in the adsorption process of heavy metals.

1.2.1.2. Pumpkin peels.

Although pumpkin peels are studied to a lesser extent than potato peels, there is some information regarding the general composition of pumpkin peels. In addition, there is slightly varying results in terms of the percent composition of complex macromolecules in pumpkin peels [23]. One study showed that when the moisture percentage was minimized to 9.76% in pumpkin peel powder, the composition resulted in 10.65% ash, 6.57% fat, 29.62% fiber, and 23.95% protein [24]. It was also shown that pumpkin peels contain a significant amount of ascorbic acid and other phenolic compounds such as gallic acid [25].

1.2.2. Adsorption Theory

Adsorption occurs when an atom, ion, or molecule adhere to the surface of an adsorbent material following physical contact [26]. Generally, adsorption can occur either through physisorption or chemisorption. Physisorption, also known as van der Waals adsorption, is a type of physical adsorption process where the atom, ion, or molecule is attracted to the surface of an adsorbent through intermolecular forces [27]. On the other hand, chemisorption is a chemical adsorption process whereby the adsorbate forms a chemical bond with the adsorbent material such as ion-exchange or complexing [28]. Due to the sharing of electrons involved in chemical bonds, the chemisorption process is more selective and stronger than physical adsorption and requires a higher activation energy to adsorb [29]. Figure 1 below illustrates the various mechanisms by which heavy metals may adsorb onto biosorbent materials.

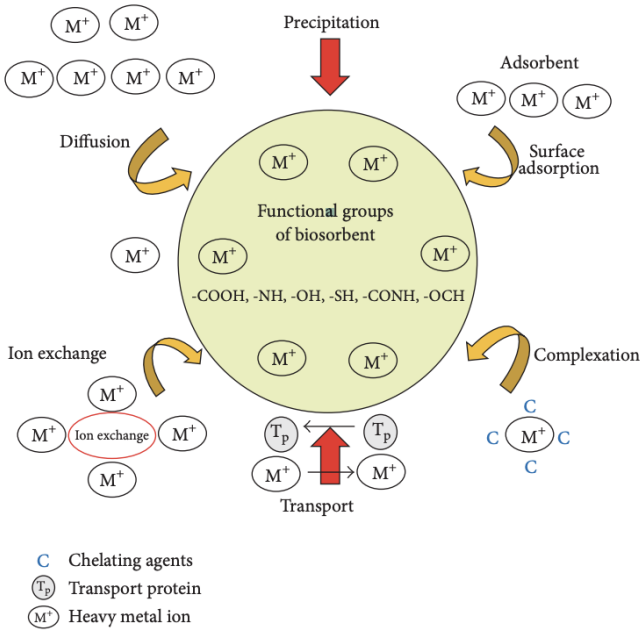

Figure 1. Biosorbent mechanisms. [30]

First, metal ions diffuse on to the sorbent surface due to concentration gradient, all the adsorption processes will depend on the mass transfer rates and the solid-liquid equilibria. The mass transfer rate depends on the type of ions or molecules, the temperature, the viscosity of the liquid, and the pore sizes of the adsorbent [30]. These adsorption processes can be explained mathematically through adsorption models known as the Langmuir and Freundlich isotherms.

1.2.2.1. Langmuir Adsorption Isotherm

The Langmuir adsorption isotherm was proposed by Irving Langmuir in 1918 based on the kinetic theory of gases [31]. The Langmuir model makes assumptions about the adsorption process that the adsorbent surface is homogeneous, sites can only adsorb one molecule at a time, adsorption occurs in one layer of the adsorbent, and no interactions occur between adsorbed material [32]. The Langmuir isotherm can be written as [33]:

$$\frac{C_e}{q_e} = \frac{1}{K_L q_0} + \frac{C_e}{q_0} \quad (1)$$

Where C_e is the equilibrium concentration of the adsorbate, Q is the mass ratio between the number of adsorbed species and the amount of adsorbent in mg/g, and K_L is the Langmuir constant expressed in L/mg.

1.2.2.2. Freundlich Adsorption Isotherm

Proposed by Herbert Freundlich in 1909, the Freundlich adsorption isotherm is an empirical model that describes the adsorption process in a heterogenous surface [34]. One limitation of this model is that it is only valid at low concentrations [35]. However, this is not a problem for studying adsorption for decontamination of water as heavy metals are

present at lower concentrations in drinking water. The Freundlich isotherm equation is shown in equation (5) in section 2.4.

1.3. ION-SELECTIVE ELECTRODES

An Ion-Selective Electrode (ISE) is an electrochemical sensor used to measure the activity of a certain ion within a sample solution [36]. The components of an ISE consist of a galvanic half-cell that comprises of an ion-selective membrane and an internal solution, and an internal reference electrode. The figure below illustrates the components of a typical ISE.

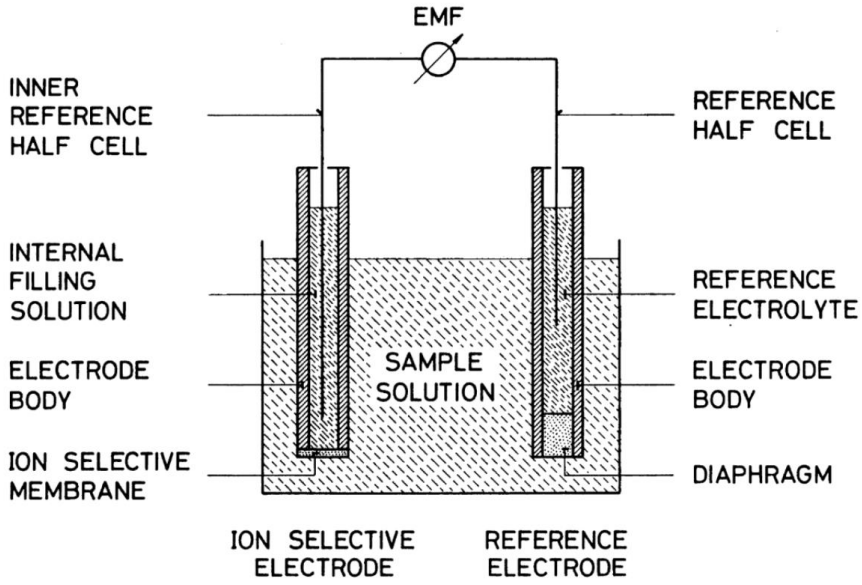

Figure 2. Schematic Diagram of an Ion-Selective Electrode [36].

A voltmeter can convert the ionic activity measurement into a potential reading using the Nernst equation. The equation below shows the relationship between the potential difference and the ionic activity provided by the Nernst equation [37].

$$E_{sample} = E_0 + \left(\frac{2.3RT}{nF}\right) * \log(a_{ion}) \quad (2)$$

Where E_0 is the standard cell potential calculated through the sum of the reference electrode potential (E_{ref}), the standard indicator electrode potential (E^0_{ind}), and the liquid junction potential for the reference electrode (E_j), R is the gas constant, T is the temperature in Kelvin, n is the charge of the measured ion, F is the Faraday constant, and a_{ion} is the activity of the specific ion being measured.

1.3.1. pH Electrodes

One of the most common methods of determining the pH of a solution is using the pH electrode. pH electrodes provide a highly reliable and accurate determination of the hydrogen ion activity within a sample. Although there are multiple methods of determining the hydrogen ion concentration in a solution, the pH electrode remains the most common and effective method of determination [38].

Although there are various types of pH electrodes, they all share common components that are crucial to making pH measurements. The first major component is the sensor, where a glass bulb on the tip of the probe is only sensitive to hydrogen ions and provides a voltage response that is directly proportional to the amount of hydrogen ions present within the sample. The other major component is a reference part. This component provides a reference voltage value to compare and validate the measurement of the sample [39]. The electrode typically contains a reference solution of known concentration and thus, known voltage reading. Both components connect to a pH meter that evaluates and automatically calculates the voltage difference between the sample and reference reading that is displayed on the pH meter screen.

1.3.2. Cadmium and Lead Ion Selective Electrodes

Cd (II) and Pb (II) ion selective electrodes operate under the same principles as pH electrodes but are designed to respond to the activity of cadmium and lead ions. Both electrodes are very similar in structure and their components is illustrated in Figure 3 shown below.

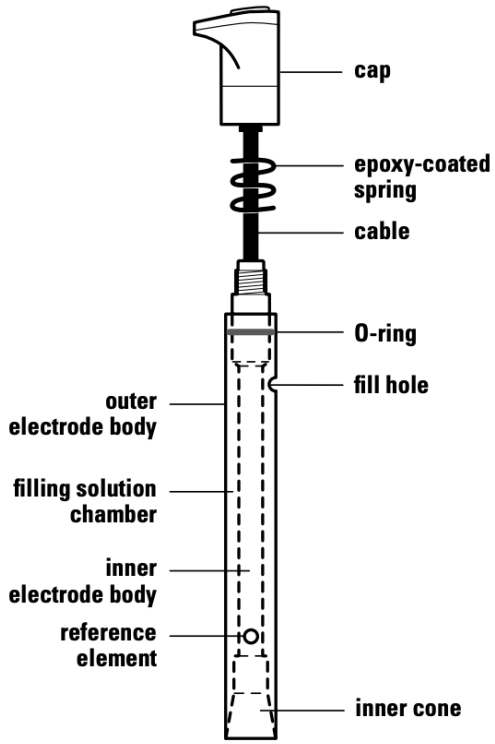

Figure 3. Structure of a Pb (II) or Cd (II) ISE [40,41].

Although the general design of both electrodes is very similar, one major difference is the specific components used in the sensing membrane [42,43]. The specific components in the membrane of an ISE are designed to bind to the ion of interest with high selectivity. The activity of the ion of interest can be measured by comparing the

known concentration in the internal filling solution to the number of ions bound to the outer sensing membrane in the sample solution [44].

Materials used in the sensing membrane of the cadmium ion selective electrode are CdS/Ag_2S solid, which have low solubility and a high specificity towards cadmium cations. The purpose of adding Ag_2S is to increase the conductivity of the solid membrane. CdS dissociation generates the membrane potential, which will depend on the Cd^{2+} or S^{2-} ion concentrations [45]. Thus, other ions may interfere by forming more insoluble compounds with the sensing membrane and generate a response. However, these ions must be present at a high concentration to exhibit a response with the cadmium-selective electrode.

Similarly, materials used specifically for lead ions in the lead ion selective electrode are PbS and Ag_2S, which also show responses to interfering ions [45]. Other lead-specific sensing membrane materials are still being tested and optimized for better performance of the electrode [46].

The pH of the solution plays an important role in the measurement of lead and cadmium ions using ion-selective electrodes. A high concentration of cadmium ions in a solution of high pH can lead to a reaction that produces cadmium hydroxide which interferes with the ISE measurement [43]. Figure 4 shows a graph of Cd (II)-ISE potential vs solution pH with varying concentrations of cadmium ions.

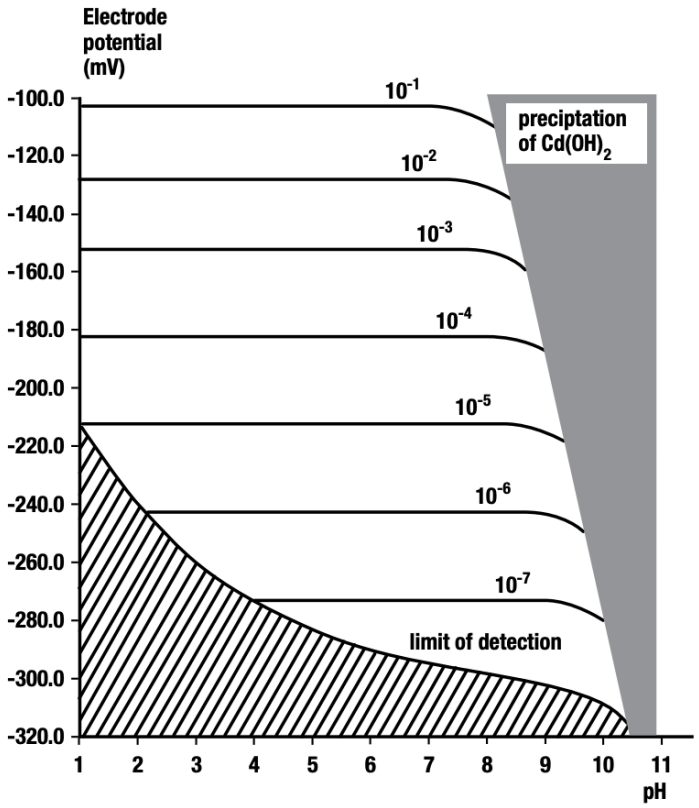

Figure 4. Electrode Potential vs Solution pH in Cadmium Ion Solutions at 25 °C. [41]

Lead ions have an even greater affinity than cadmium ions to react in aqueous solutions to produce lead hydroxide. As shown in figure 5, lead hydroxide can precipitate even at a pH value of 7. Thus, it is important to use a lower concentration of lead ions or a buffered solution to make accurate lead ion measurements using a Pb (II)-ISE.

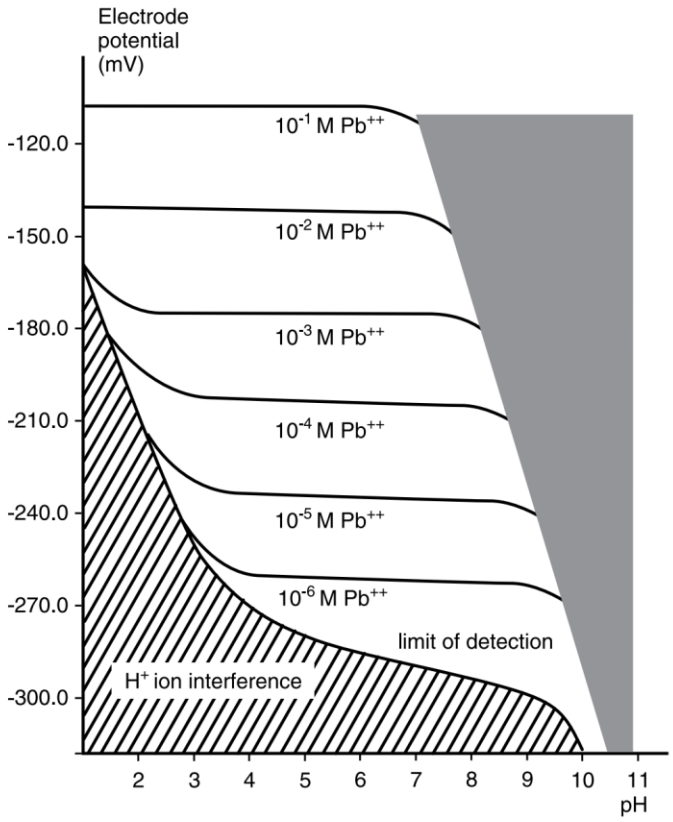

Figure 5. Electrode Potential vs Solution pH in Lead Ion Solutions at 25 °C [42].

1.4. INDUCTIVELY COUPLED PLASMA OPTICAL EMISSION SPECTROSCOPY

Inductively Coupled Plasma Optical Emission Spectroscopy (ICP-OES) is an analytical tool used to determine the elemental composition within a sample. As opposed to other ICP methods, ICP-OES utilizes emission spectroscopy where a high temperature plasma produces excited atoms and ions that emit radiation corresponding to a particular element [47].

In ICP-OES, the sample is initially nebulized into fine aerosol droplets that are directed into a hot plasma [48]. The plasma is generated by argon gas and can reach extremely high temperatures that atomize and ionize the sample [49]. The excited atoms

and ions, upon their return to the ground state, emit light at characteristic wavelengths corresponding to particular element that pass through a spectrometer. The emitted light is then dispersed into their component wavelengths where their intensity is proportional to the concentration of the element within the sample [50].

The ICP-OES instrument can cover a large range of concentrations depending on the instrument used and the element being analyzed. Most often, the detection limit for the instrument can be as low as 0.1 parts-per-billion (ppb) and can cover concentrations up to 1000 parts-per-million (ppm) [51]. It is most common for this instrument to analyze samples in liquid form but may be able to analyze gases in some cases [52]. It is also important to filter and treat the samples prior to analysis with the ICP instrument with nitric acid to stabilize the elements being analyzed. Nitric acid, being a strong acid, can stabilize the heavy metals to prevent precipitation with hydroxide ions and adsorbing onto the walls of the sample container when analyzing the sample [53]. It also provides a more uniform solvent background, enhancing the introduction of liquid samples into the ICP torch by promoting the formation of smaller, more consistent droplets. In addition, the nitric acid pretreatment may serve to digest solid samples and aids in cleaning the instrument to prevent cross-contamination between samples [54].

Although the ICP-OES instrument is highly sensitive and has a wide range of applications, it is extremely costly and requires expert handling for proper management and measurements. This may be a disadvantage for certain experiments that may hinder the advancement of future adsorption studies.

1.5. INFRARED SPECTROSCOPY

Fourier Transform Infrared Spectroscopy (FTIR) is a widely used analytical technique to identify prominent functional groups in molecules. Its principle is based on the use of infrared light interacting with different parts of a molecule through absorption, emission, photoconduction, or Raman scattering to create various signals in an infrared spectrum [55].

The process of FTIR analysis starts with an infrared light source sending an array of various frequencies into the sample compartment where different parts of the molecules interact with different frequencies of the infrared light. Depending on the functional groups and type of bonds contained within the sample, a signal will be obtained when the frequency of the light source matches the vibrational frequency of the bond that leads to absorption [56].

In an FTIR spectrum, the graph is plotted as transmittance percentage (%T) versus wavenumber (cm^{-1}) where the wavenumber corresponds to the frequency of the light source. When a signal is obtained, a decrease in the transmittance of light is observed as the bonds in the molecule absorb some of the light and lead to a lower transmittance relative to the light source [57]. Each molecule contains a unique FTIR spectrum and can be identified through its fingerprint region in the 400-1200 cm^{-1} area. Figure 6 shows an example of an FTIR spectrum for the glucose molecule.

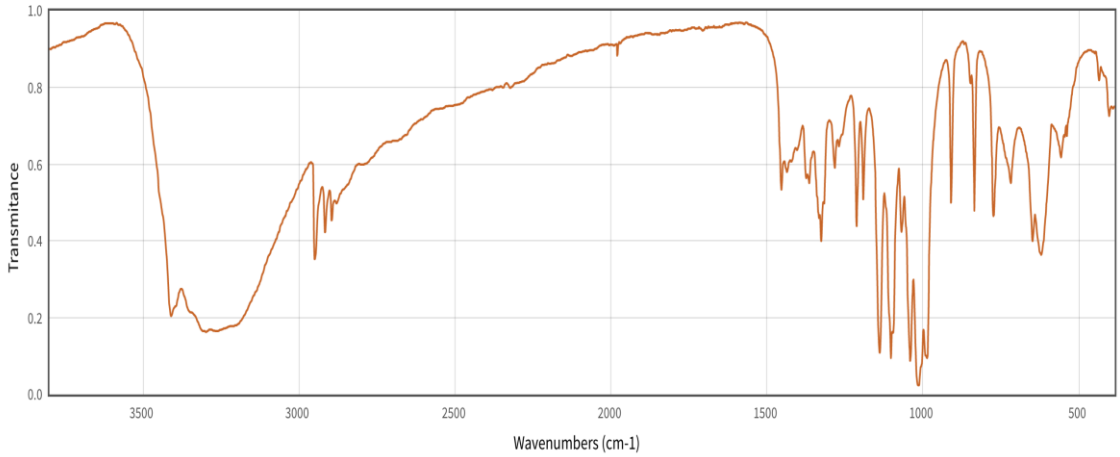

Figure 6. FTIR spectrum of D-glucose [58].

1.6. SCANNING ELECTRON MICROSCOPY

Scanning Electron Microscopy (SEM) is a type of electron microscopy that uses beams of electrons to produce a microscopic image of a sample surface. The main components of an SEM instruments consist of an electron gun to generate high energy electrons, a column containing electromagnetic lenses to focus the electrons in a specific area of the sample, a sample chamber, an electron detector for emitted electrons, and a computer system to analyze the images produced [59].

The electron gun produces an electron beam by heating a tungsten wire where the high energy electrons are generated and travel into a vacuum column. The column focuses the electron beam into a specific part of the sample using electromagnetic lenses. The magnification of the image provided can be altered using a computer system by focusing the electron beam into a smaller or greater area of the sample [60]. Once the beam touches the surface of the sample, signals are produced through emission of various signals such as secondary electrons, Auger electrons, back scattered electrons,

characteristic X-rays, and cathodoluminescence [61]. These signals are then trapped by detectors and converted into a digital image in a connected computer system that allows for analysis of the sample's morphological and structural composition.

1.7. CURRENT RESEARCH AND OBJECTIVES

Currently, the metal ion concentration determination methods used in the adsorption of metal ion studies are mostly based on the atomic spectroscopy, atomic absorption (AAS), and inductively coupled plasma atomic emission (ICP-AES/OES) [18-19,62-64]. Compared to spectroscopic methods, electrochemical methods [65,66] require inexpensive and smaller equipment. Ion-selective electrodes (ISE) offer further advantages such as measuring free ion activity, and in-situ continuous monitoring without sample pre-treatment [67-69]. This is especially convenient for kinetic studies with multi-phase systems, without separation to monitor the free ion concentration/activity during adsorption. This work shows that a commercial solid-state ion-selective electrode for Cd (II) and Pb (II) work satisfactorily in following the free concentration change during the adsorption process. Pumpkin and potato peels were selected as sorbents due to their high availability and the base treated sorbents showed high adsorption to cadmium at higher pH values. Fixed bed column adsorption of cadmium was also performed to evaluate the dynamic adsorption of cadmium for water treatment and sorbent reuse when regenerated with nitric acid.

This research serves to provide viable and cost-effective methods for the process of decontaminating water from cadmium and lead. Although research in adsorption of heavy metals using biowaste sorbents has been performed previously, there is little focus on cadmium ions in water as well as little to no research done on pumpkin peels.

In addition, another important objective is to provide a cheap and reliable way to perform measurements of heavy metal adsorption without sacrificing accuracy. Thus, we will be comparing and analyzing the lead and cadmium adsorption capacities of biowaste sorbents between the expensive ICP-OES instrument and the relatively cheaper ISE method.

Accurate measurements of adsorption capacities using electrodes provide many benefits to the environmental field. The use of ISE to assess water decontamination will allow more access to this field of research where various biowaste sorbents can be analyzed and potentially used to extract heavy metals from contaminated water.

CHAPTER 2:

MATERIALS AND METHODS

2.1. CHEMICALS AND REAGENTS

All solutions were made and diluted using Ultrapure (UP) deionized water obtained from a Direct-Q 3 UV-R purification system with a product resistivity of 18.2 M Ω·cm at 25 °C.

2.1.1. Metal Ion Solutions

Cadmium chloride 1.5 hydrate with a purity of 97% was purchased from Millipore Sigma. A stock solution of 880 ppm of cadmium ion solution was prepared by adding 1.647 g of cadmium chloride 1.5 hydrate in a 1L volumetric flask with UP deionized water. Using the stock solution, serial dilutions were made to make 440, 220, 88, 44, and 8.8 ppm of cadmium ion solutions.

Lead (II) nitrate crystals with a purity of 99% were purchased from JT Baker Chemicals. A stock solution containing 1000 ppm of lead ions was prepared by adding 1.598 g of lead (II) nitrate to a 1L volumetric flask with UP deionized water. Successive dilutions were followed to make 500, 250, 100, and 50 ppm solutions of lead ions.

2.1.2. Buffer Solutions

ACS grade glacial acetic acid and solid sodium acetate were purchased from JT Baker Chemicals. To prepare a 0.1M acetic acid/acetate buffer solution, 800 mL of UP deionized water was added to a 1-liter volumetric flask. Then, 340 microliters of glacial acetic acid and 7.7 grams of sodium acetate with added to the volumetric flask and mixed thoroughly. The pH was measured and adjusted accordingly using either acetic acid or

sodium acetate to reach a pH of 5.6. UP deionized water was finally added for the volumetric flask to reach 1 liter and the flask was mixed and ready for use.

Tris(hydroxymethyl)aminomethane, sodium chloride, and potassium chloride were all purchased from JT Baker Chemicals and were used to make a tris buffer of pH 7.4. The buffer was made in a similar manner to the acetic acid/acetate buffer by adding 800 mL of UP deionized water to a 1-liter volumetric flask. Then, 12 grams of tris(hydroxymethyl)aminomethane along with 0.2 grams of potassium chloride and 8 grams of sodium chloride were all added to the volumetric flask. The pH was measured again and adjusted accordingly with hydrochloric acid to reach a final pH of 7.4. This buffer was only used for the cadmium solutions as the lead solutions precipitated at any pH above 7. For lead solutions, the acetic acid/acetate buffer was used for all measurements.

2.2. INSTRUMENTATION

2.2.1. Ion-Selective Electrodes

All ISEs in this study used the Thermo Scientific Orion STAR A112 pH-meter. The pH meter was calibrated using buffer solutions made by Thermo Scientific. 60 mL bottles were purchased of pH values 4.00, 7.00, and 10.01 and were used to properly calibrate pH meters on a weekly basis.

A ROSS ultra-combination electrode was used to make pH measurements. A cadmium combination ion-selective electrode (Orion, ionplus sure-flow solid state, 9648BNWP) was used for measurements of cadmium concentrations and was purchased from Thermo Scientific. A lead half-cell electrode (Orion, ionplus sureflow, 9482BN) was used for measurements of lead concentrations and was also purchased from Thermo

Scientific. For lead measurements, the lead ISE was used in combination with a double junction reference electrode with both electrodes embedded within the sample solution for all measurements.

2.2.2. FTIR

FTIR analysis was performed using a Perkin Elmer Spectrum 100 FTIR spectrometer (LR 64912C) with a diamond-attenuated total reflectance (ATR) accessory. Measurements were taken with 4 scans at 1 cm^{-1} resolutions and were recorded within the 4000–650−cm^{-1} region. A background measurement of air was taken before every first measurement of the day. In between each measurement, the sample compartment was cleaned using an acetone-dipped Q-tip and left to dry for at least 30 seconds.

2.2.3. ICP-OES

Cadmium and lead ion concentrations were also measured using a Perkin Elmer ICP Optical Emission Spectrometer (Optima 2100DV ICP-OES). The wavelengths used for lead and cadmium measurements were 220.353 nm and 228.802 nm, respectively.

2.3. BIOWASTE SORBENTS

Potatoes and pumpkins were ordinary kinds obtained from New York City stores. Their peels were collected, rinsed with tap water, then with distilled water several times and air dried for three days at ambient conditions. The dried peels were hand-milled in a mortar and pestle and sieved through an 18-mesh sieve. To find the best adsorption conditions, biosorbents were treated with acid or base. Their treatment was done by adding 7.5 g of the biosorbent to 200 mL of 0.4 M HNO_3 or NaOH. The mixture was left for 24 hours, and then filtered with filter paper and the solid biosorbents were collected. The material was left to air dry in the laboratory for 3 to 5 days before use.

2.4. BATCH EXPERIMENTS

Adsorption experiments were performed on base treated biowaste substrate. The adsorption study was performed in isothermal conditions at 20 ± 2 ^{o}C for 24 h using batch equilibration procedure by treating 0.100 or 0.200 g of the substrate with equal volume of increasing Cd (II) concentrations (8.8 to 880 ppm) in buffered or non-buffered solutions while stirring for the first 2 hours. After 24 hours, the pH and equilibrium concentration were measured with the cadmium combination electrode (Cd (II)-ISE) for Cd (II) ion adsorption or lead combination electrode (Pb (II)-ISE) for Pb (II) ion adsorption with a Thermo Scientific Orion STAR A112 pH-meter. For unbuffered adsorption experiments, 5.0 mL of unfiltered solution was mixed with 5 mL of 0.1 M acetic acid buffer (pH 5.6) for a fixed pH and ionic strength ISE measurement. The remaining supernatant solutions of some selected sets were filtered with regular filter paper, and then with a 0.45 mm HPLC filter paper. 5.00 mL of the filtered solution was mixed with 5.00 mL of 4% nitric acid for the atomic emission measurements. Cd (II) and Pb (II) ion concentrations were also measured with an ICP optical emission spectrometer at 228.802 and 220.353 nm, respectively.

Adsorption efficiency (A%) was calculated with equation (3) with the initial concentration introduced into the solution C_0 and equilibrium concentration (C_{eq}). The adsorption isotherms were obtained by plotting the amount of Cd adsorbed (Qe, equation 4) against the C_{eq} in the solution with the linear form (equation 6) of the Freundlich equation (5) [68].

$$\%A = \frac{C_0 - C_{eq}}{C_0}\% \tag{3}$$

$$Q_e = \frac{(C_0 - C_e)V}{w} \quad (4)$$

$$(Q_e) = K_f \times C_{eq}^{1/n} \quad (5)$$

$$log(Q_e) = logK_f + \frac{1}{n} logC_{eq} \quad (6)$$

Where (Q_e) is the mass ratio between the amount of adsorbed species and the amount of adsorbent (w), V is the volume of the aqueous solution, K_f and 1/n are constants which represent the adsorption capacity and the adsorption intensity respectively. By plotting log Q_e *vs* log C_{eq}, the linear correlation coefficient, R can be quantified. Significant linearity was tested according to the significance statistical test for the R coefficient [67]. The K_f constant (adsorption capacity) is given by the intercept and n value is given by the slope.

2.5. ADSORPTION KINETICS

Kinetics studies were performed in batch mode with 0.100 g of substrate and 20 ml of various initial metal ion concentrations under constant stirring for up to two hours. The pH and the ISE potential were continuously recorded. The final concentration after 24 hours was measured again with metal ion selective electrode and ICP-OES. The kinetics of adsorption was fitted with the pseudo-second order model using the following equation:

$$Q_t = \frac{(C_0 - C_t)V}{w} \quad (7)$$

$$\frac{t}{Q_t} = \frac{1}{K_2 Q_e^2} + \frac{t}{Q_e} \quad (8)$$

Where C_t is the concentration of the heavy metal ion measured with the ISE and, Q_t is the mass ratio at time t. K_2 is the second-order adsorption rate constant in g mg^{-1} min^{-1} computed from the linear plot of t/Q_t versus t. Q_e can be calculated with the slope, Q_e=1/slope. The rate constant is calculated as: $K_2 = 1/ (\text{intercept} \times Q_e^2)$ with units of g mg^{-1} min^{-1}.

2.6. DYNAMIC ADSORPTION AND DESORPTION/RECOVERY OF THE BIOSORBENTS

Waste treatment-dynamic adsorption of cadmium from aqueous solution was carried out as follows. Six grams of ground pumpkin peel was placed in a flash chromatography column tube, soaked in 170 mL of 0.4 M NaOH overnight, drained, washed with 200 mL of ultra-pure water and subsequently drained. A solution of 220 ppm of cadmium was added continuously with a draining speed of 2 mL/min. The draining solution was collected in 50- (in the beginning) or 20 mL (after 400 mL) beaker batches and monitored with a cadmium ion-selective electrode and pH electrode; the process is stopped when the Cd (II)-ISE showed significant potential increase.

The biosorbent was then regenerated with 800 mL of 0.4 M HNO_3, slowly drained, and washed with 800 mL of ultra-pure water, to obtain neutral pH of the draining solution. The process of cadmium adsorption was repeated using a 200 ppm Cd solution in dilute Tris-HNO_3 buffer of pH 7.2 for a pH control. Cadmium adsorption-regeneration was repeated 3 times to evaluate the regeneration efficacy.

CHAPTER 3:

RESULTS AND DISCUSSION

3.1. CALIBRATION CURVES

Calibration methods were performed for lead and cadmium on both ICP-OES and the respective ion-selective electrodes. Figure 7 shows two calibration curves obtained from ICP-OES. Figure 7(a) shows the calibration curve for cadmium quantification at 228.802 nm in 2% nitric acid while figure 7(b) is for lead quantification at 220.353 nm in 2% nitric acid with ICP-OES. Both curves present high linearity within the concentration range.

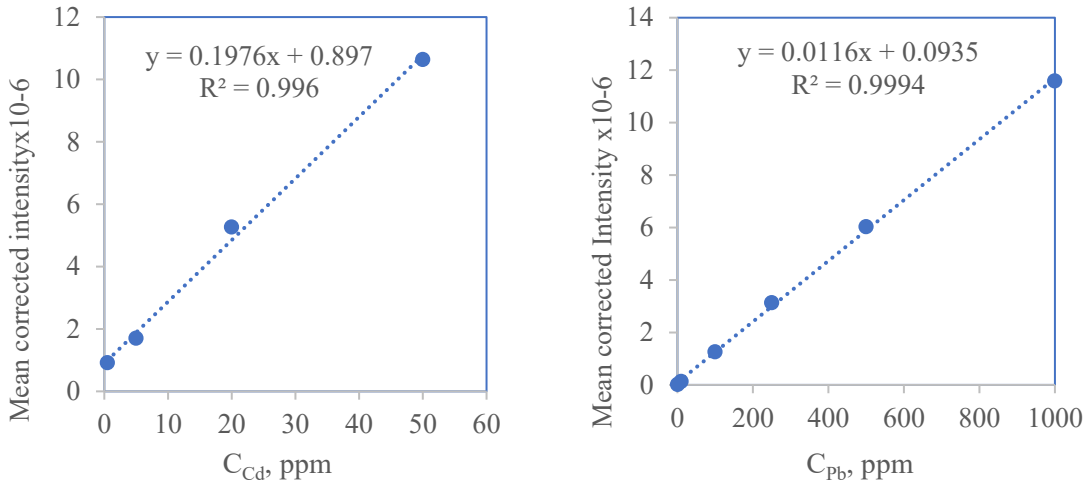

(a) (b)

Figure 7. Calibration curves for (a) Cd and (b) Pb with ICP-OES in 2% nitric acid.

Figures 8 (a) and 8 (b) show the graphs of cadmium and lead ion-selective electrodes calibration curves at a pH of 5.6 in acetic acid buffer. After two weeks of use, the electrode slopes are shown to be slightly below the manufacture certified calibration

value of 27±2 mV/dec at 22 ºC. However, a wide response range is used for both electrodes to measure a wider range of concentrations of these ions through adsorption by the biosorbents.

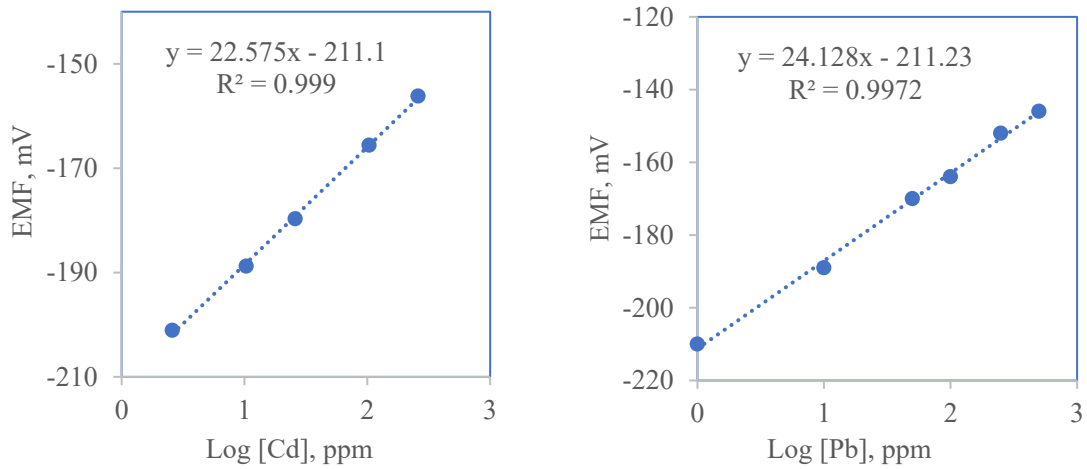

(a) (b)

Figure 8. Calibration curves for (a) Cd (II) and (b) Pb (II) ion-selective electrodes in acetic acid buffer, pH 5.6.

Table 1 below summarizes the calibration curve equations and relevant statistics for lead and cadmium from both ICP-OES and ISE for comparison.

Table 1. Calibration statistics for ICP-OES and ion-selective electrodes.

Method	Equation	R^2	Range (ppm)
Cd-ICP at 228.702 nm	$I = [0.1976[Cd] + 0.897]x10^6$	0.996	0-50
Pb-ICP at 220.353 nm	$I = [0.0116[Pb] + 0.0935]x10^6$	0.999	0-1000
Cd (II)-ISE	E = 22.6log [Cd] – 211.1	0.999	0-500
Pb (II) -ISE	E = 24.1log [Pb] – 211.2	0.997	0-500

3.2. PRELIMINARY RESULTS

Various biowaste sorbent materials were screened to assess their efficacy in adsorbing cadmium and lead ions. These adsorbents include ground coffee beans, crushed peanut shells, sunflower shells, chamomile tea leaves, pumpkin peels, and potato peels. The table below shows the adsorption efficiency for these sorbents in adsorbing cadmium ions.

Table 2. Sorbent Screening using Cd(II)-ISE with 220 ppm Cd(II) solutions over 2 hours for various biosorbents.

Sorbent	Ground Coffee Beans	Crushed Peanut Shells	Sunflower Shells	Chamomile Tea Leaves	Potato Peels	Pumpkin Peels
EMF change (mV)	-8	-19	-23	-23	-105	-120
%A	50	81	87	87	99	99

Both potato peels and pumpkin peels show excellent adsorption efficiencies with cadmium ions and were further analyzed in more detail to understand the adsorption mechanisms in adsorbing cadmium and lead ions.

3.3. BIOSORBENT CHARACTERIZATION

3.3.1. FTIR

Fourier transform infrared analysis in solid phase before and after metal ion adsorption was performed and analyzed to find differences in biosorbent characteristics. The FTIR Spectra of pumpkin peel sorbent before and after lead ion adsorption is shown in Figure 9. The pumpkin peel showed peaks for O-H and N-H groups at 3600-3000 cm^{-1} range, C-H at 2918 and 2850, C=O group at 1733, C=C at 1634, C-O at 1238, C-N at 1015 cm^{-1}.

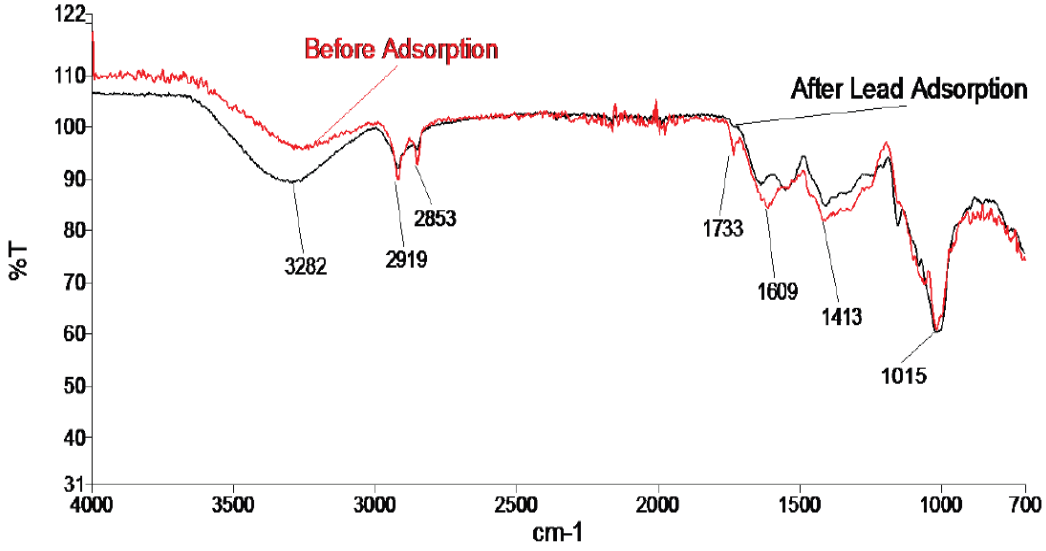

Figure 9. FTIR spectra of base treated pumpkin peel before and after Pb (II) adsorption.

Figure 10 shows the FTIR spectrum of pumpkin peels before and after cadmium adsorption. The characteristic peaks of the pumpkin peels analyzed for cadmium adsorption are O-H and N-H groups at 3600-3000 cm^{-1} range, C-H at 2921 and 2851 cm^{-1}, C=N, C=C at 1611 cm^{-1}, C-H, O-H at 1413 cm^{-1}, C-C, C-N at 1013 cm^{-1}, and C=O at 1733 cm^{-1}. Although there are variations of the effect of lead and cadmium adsorption

within the fingerprint region of the pumpkin peel, this indicates that upon adsorption, there is a major change in the chemical composition of the pumpkin peal. However, both metal ions show that adsorption leads to a decrease in the carbonyl peak at 1733 inverse centimeters is observed. This may indicate that the functional groups C=O, C-O, C-N are some binding sites to the cadmium and lead ions.

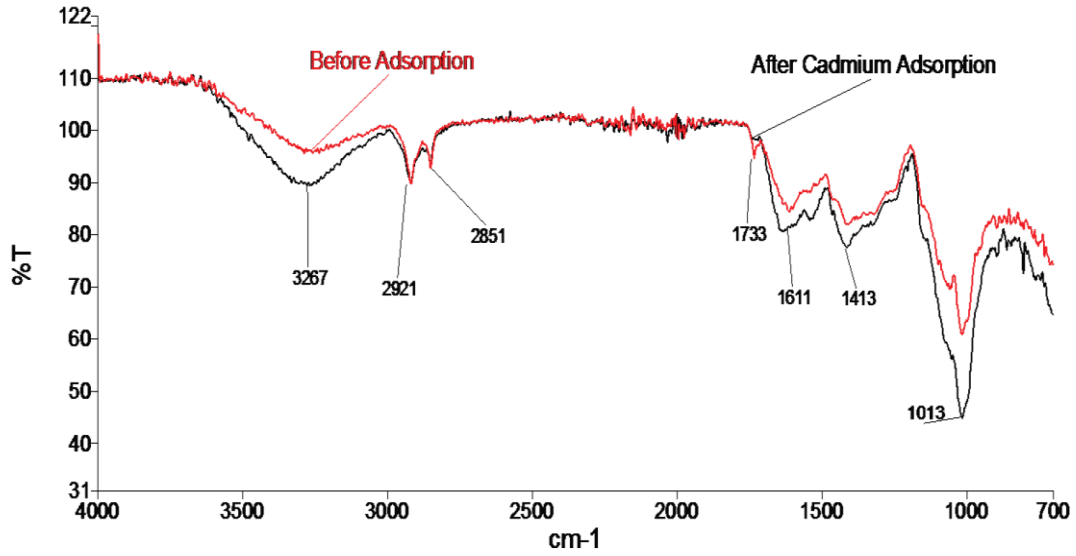

Figure 10. FTIR spectra of base treated pumpkin peel before and after Cd (II) adsorption.

FTIR spectra of potato peels were also performed but not provided in this study. Although some spectra showed a decrease in the carbonyl stretch intensity after heavy metal adsorption, the fingerprint region and other prominent peaks of potato peels were inconsistent between different measurements. This is most likely due to the composition of the potato peels and their difficulty to be ground into finer particles using a mortar and pestle to be measured more accurately in the FTIR.

3.3.2. Sorbent Morphology

Morphological analysis of the biowaste sorbents was carried out using scanning electron microscopy. Figure 11 shows the SEM images of potato peels and pumpkin peels upon base treatment.

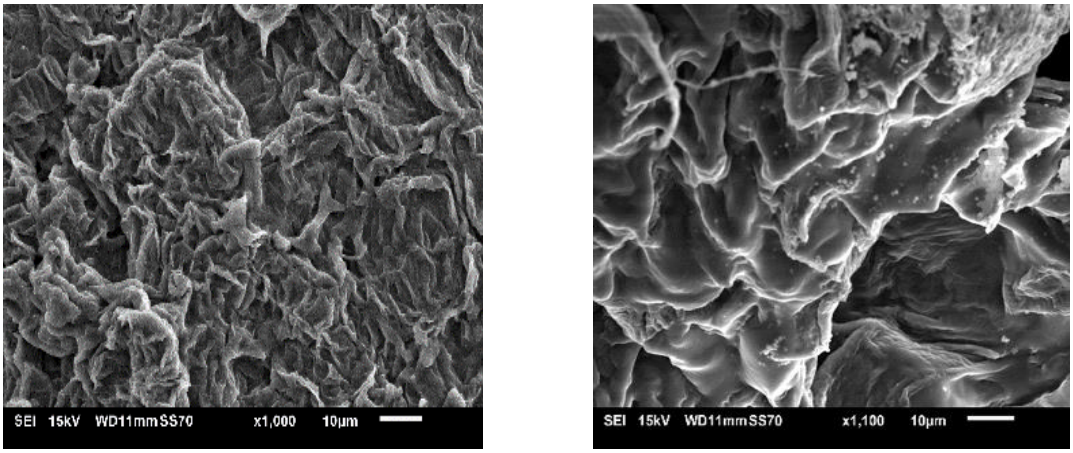

(a) (b)

Figure 11. Scanning electron microscopy of (a) pumpkin peel and (b) potato peel porous biosorbents.

The SEM images of both base treated biosorbents show a porous and heterogeneous structure upon 1000x magnification. It was also found that the bulk densities of pumpkin peels and potato peels were 0.71 and 0.41 g/cm^3, respectively.

3.4. CADMIUM ADSORPTION

3.4.1. Time response monitored with Cadmium ISE

A 20 mL solution was prepared with various cadmium concentrations with and without buffer. Upon addition of 0.100 grams of biosorbent, the electrode was placed into the solution and the potential was monitored with a pH meter continuously over the course of 120 minutes with stirring conditions.

Figure 12 (a) shows the electrode potential plotted against time after the base treated pumpkin peel sorbent was added in a non-buffered solution. There was a gradual decrease of cell potential as time progressed after the addition of the sorbent. To show that the adsorption is second order, the concentration of the cadmium ions was calculated with the calibration curve shown in Table 1, the quantity of adsorption (Q_t) at time *t* was calculated with equation (8), the t/Q_t was then plotted and is shown in Figure 12. As shown in Figure 12(b), the second order kinetic model plot has a high linearity with a R^2 of 0.999. Therefore, it is inferred that the adsorption kinetics are second order, suggesting a high degree of chemisorption in the process of cadmium adsorption.

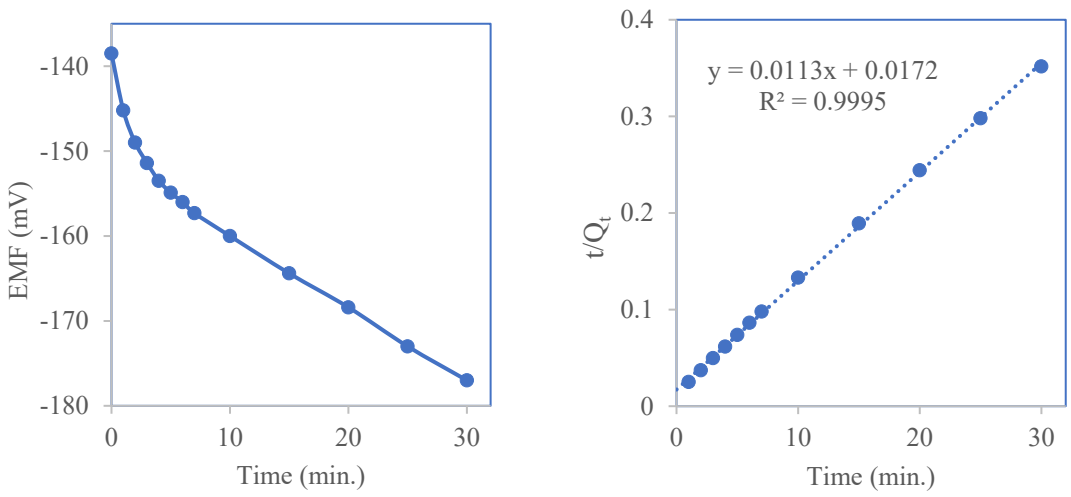

(a) (b)

Figure 12. (a) Time response of the Cd((II)-ISE with 20 mL of 440 ppm initial cadmium in water when 0.10 g of base treated pumpkin peel was added. (b) Linear plot of the second order model.

Adsorption of cadmium with pumpkin peels at a buffered pH of 5.6 showed an excellent electrode response and fitting in the second order model. Figure 13 compares the adsorption of pumpkin peels with initial cadmium concentrations of 220 and 440 ppm in buffered solutions and their linear plot of the second order model.

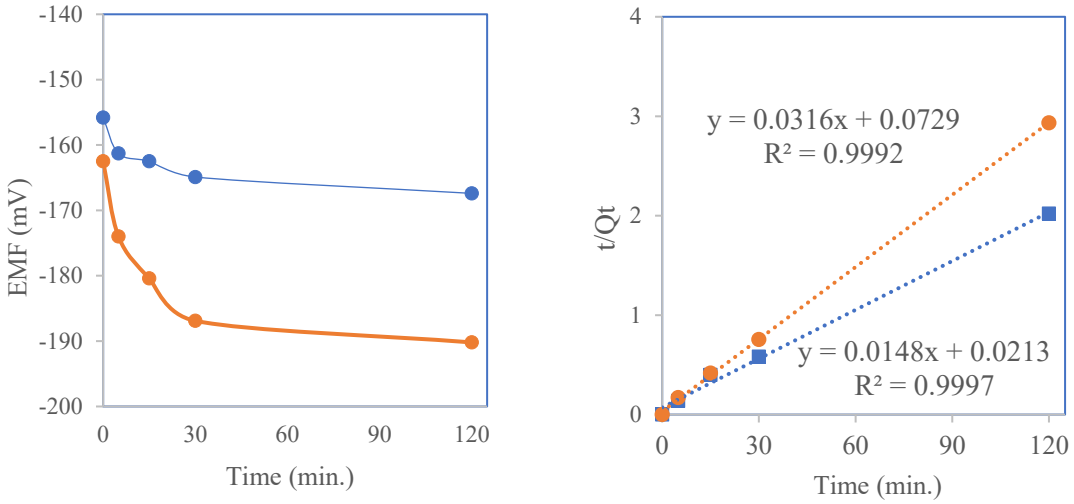

(a) (b)

Figure 13. (a) Time response of the Cd((II)-ISE with 20 mL of (▪)440 ppm, (●) 220 ppm initial cadmium in acetate buffer pH 5.6 when 0.10 g of base treated pumpkin peel was added. (b) Linear plot of the second order model.

Adsorption of cadmium by potato peels sorbent showed similar patterns to the pumpkin peel sorbent with base treatment. The kinetic adsorption at lower pH buffered solutions using base treated sorbents all showed good fitting to the second order model. Figure 14 (a) shows a time response plot with the electrode potential change over time for the potato peels sorbent in a buffered solution of pH 5.6. The initial cadmium concentrations used are 220 and 440 ppm, and both show a fast response nearing equilibrium after 30 minutes. The kinetic response was plotted in a second order model and shows excellent linearity for both initial concentrations as illustrated in figure 14 (b). As equation (8) shows, the lower initial concentration corresponds to a lower adsorption quantity Q_e and a higher slope (Figure 14b).

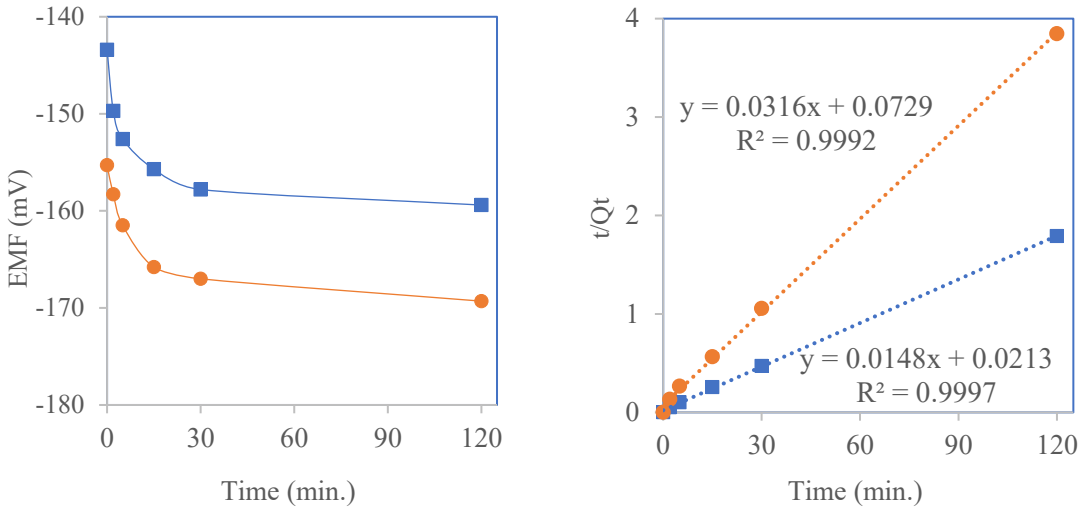

Figure 14. (a) Time response of the Cd((II)-ISE with 20 mL of (▪)440 ppm, (●) 220 ppm initial cadmium in acetate buffer pH 5.6 when 0.10 g of base treated potato peel was added. (b), Linear plot of the second order model.

The second order fitting data with an initial cadmium ion concentration of 440 ppm for both potato and pumpkin peels sorbents at three different solution pH media are summarized in Table 3. These data show that the Q_e values derived from equilibrium measured concentration (Q_e^m) are close to calculated value (Q_e^{cal}) from the second order kinetic plots. When the equilibrium concentration sets were run with ICP-OES, the Q^m values are also very close to the ISE measured values. These data results confirm that the Cd((II)-ISE measurement is accurate following the adsorption process even at the unbuffered solution. The reaction kinetic is second order confirmed also by all the linear regression R^2 values nearing unity. With high cadmium initial concentrations used, Q_e values are among the highest with the biosorbent materials reported [17,18,20,62].

Table 3. Freundlich isotherm fitting and kinetics constants for 440 ppm of Cd(II) at various sorbents measured with Cd(II)-ISE.

Sorbent	K_f	n	$Q_e^{m,ISE,ICP*}$	$Q_e^{cal\#}$	K_2	R^2
Pumpkin base-pH>8	56	6	87, 86	88	0.031	1
Pumpkin-base-pH 7.2	27	5	68	68	0.0084	0.993
Pumpkin base-pH 5.6	2.0	1.5	49	51	0.0056	0.997
Potato base-pH>8	79	12	88, 84	88	1.29	1
Potato base-pH 7.2	39	5	87	87	0.037	1
Potato base-pH 5.6	27	1.5	67	67	0.010	0.999

*: Q_e^m-ISE, ICP are the values obtained with the equilibrium concentration of 440 ppm initial concentration measured with ISE.
#: Q_e^{cal} is the value derived from the second order kinetic plot of the same initial concentration.

3.4.2. Cadmium Adsorption Isotherms

Prior to contact with cadmium, the base treated pumpkin and potato peels are basic. When no buffer is used, the pH of the sorbent-cadmium solutions at equilibrium changed significantly due to adsorption of cadmium. The higher the initial concentration was used, the lower the pH became at equilibrium. There was no precipitation observed throughout the cadmium concentration ranges used. Due to the high amount of adsorption observed in the time response analysis, much higher initial concentrations were used to obtain detectable equilibrium concentrations for both ICP-OES and ISE methods. Figure 15 shows the pH values measured after 24 hours equilibrating with different initial cadmium solutions contacting with the two sorbents.

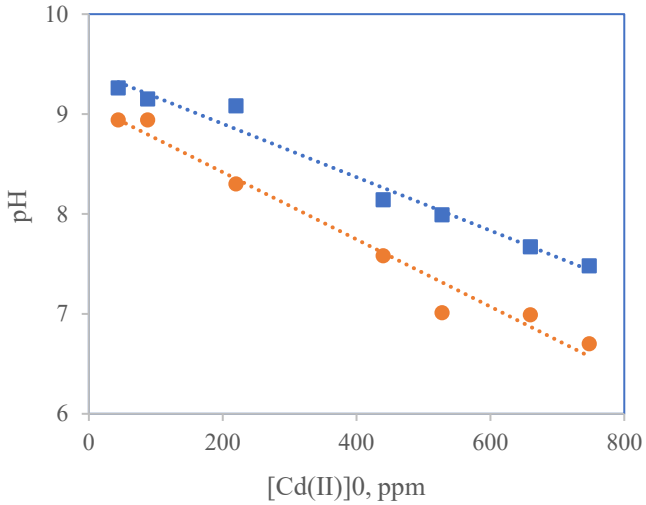

Figure 15. Variation of pH along the adsorption reaction of Cd(II) at various initial Cd(II) concentrations with base treated substrates (▪) potato peel, (●) pumpkin peel.

Figure 15 clearly shows the decrease in pH values from basic to near neutral as initial cadmium concentrations increased from 44 to 880 ppm after reaching equilibrium. The equilibrium concentration of the cadmium measured with the ISE again when the solution was mixed with acetic acid buffer of pH 5.6 and ICP-OES all show there was a great reduction in the cadmium concentration. The decrease of pH may be a result in the cation-exchange with sodium or hydrogen at various anion sites: e.g., COO^-, O^- [18]. This result is consistent with the FTIR results showing a reduced intensity signal of the carbonyl stretch at 1733 cm as deprotonation of the sorbent leads to resonance structures that reduce the intensity of the carbonyl functional groups.

Equilibrium studies were also carried out for cadmium adsorption in buffered conditions lower pH values of 7.2 and 5.6 with the Cd (II)-ISE and pH electrodes on the two sorbents to observe the pH effects. In the buffered media, the pH of the solution

changed less than -0.2 pH units with all the initial cadmium concentrations. The isotherms all showed an L-shape and fit well on the Freundlich model. Table 3 also presents the isotherm studies for cadmium adsorption in various solution media. Along with the kinetic values at the same initial concentration, these data show that the adsorption is higher at higher pH as indicated with the higher amount of cadmium adsorbed (Q_e), adsorption capacity (K_f), and adsorption rate constant (K_2). The effect of pH clearly suggests that the cation-proton exchange is a key factor in the cadmium adsorption as suggested by previous research [18].

For ICP-OES, the lower initial cadmium concentrations measured were undetectable as adsorption led to an even lower concentration. Thus, isotherms are calculated only using the last four points that are shown in Figure 16 (a) using the concentrations 880, 440, 220, and 88 ppm. Figure 16 (b) shows the Freundlich model, and the linear fitting shows a better correlation with both biosorbents.

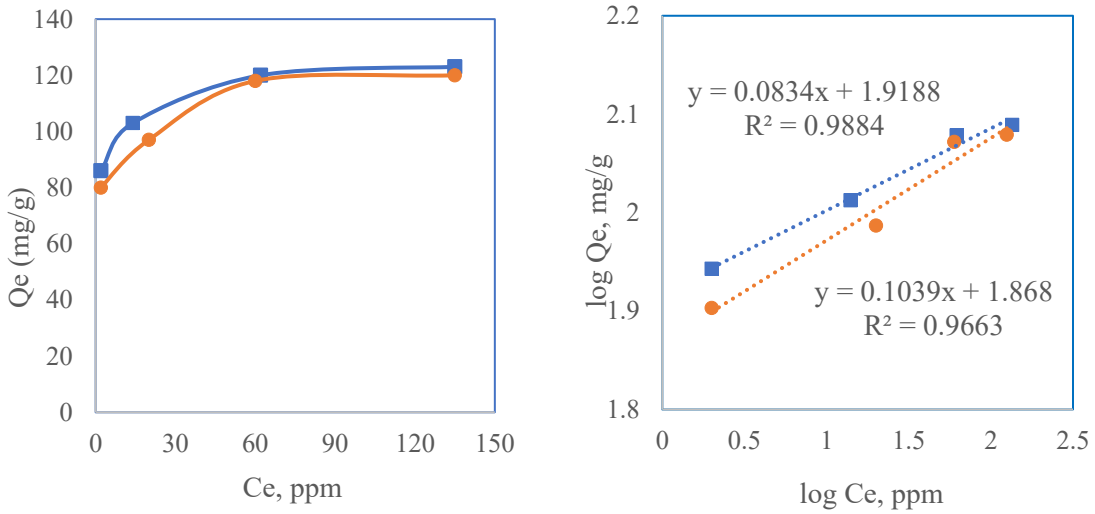

(a) (b)

Figure 16. (a) Adsorption isotherm and (b) Freundlich fitting equations for Cd(II) adsorption on base treated (▪) potato and (●) pumpkin peel biosorbents.

Both ICP and ISE methods fit the Freundlich model well and show very similar L-shaped isotherm curves. Figure 17 below compares the adsorption isotherms and Freundlich fitting equations for Cd (II) adsorption using ICP-OES and Cd (II)-ISE. The isotherms measured with the two methods show high resemblance.

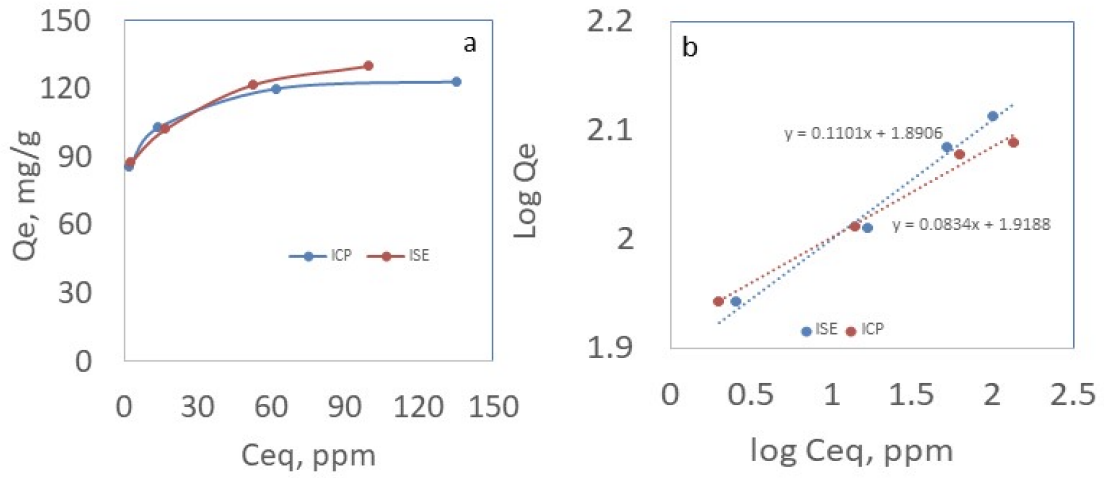

(a) (b)

Figure 17. Adsorption isotherms and Freundlich fitting equations for Cd (II) adsorption on base treated potato sorbents using equilibrium concentrations measured with ICP and ISE.

3.4.3. Column adsorption of cadmium

6.0 g of ground pumpkin was introduced into a flash chromatography column with a porous frit at the bottom. To perform base treatment, 200 mL of 0.4 M NaOH was applied to the column and kept for 24 hours before it was drained and washed with 50 mL of water. Then, 220 ppm Cd (II) in dilute acetic acid buffer was introduced into the column. At a draining speed of 2 mL/min, the electrode potential remained at a blank value until 460 mL of draining solution was collected. This corresponds to 101.2 mg of cadmium that was adsorbed onto the 6 g of sorbent, which gives a 16.9 mg/g capacity.

The column was then regenerated by introducing 300 mL of 2% nitric acid, with a draining speed of 1 mL/min. followed by washing with water until the pH was observed to be neutral with pH paper. 200 ppm of Cd (II) solution in dilute Tris-HNO_3 solution was introduced. Draining at a speed of 1-2 mL/min., the regenerated sorbent gives 15.0

and 15.4 mg/g capacity the second and third time. Figure 18 shows the potential of the cadmium electrode (a) and the pH (b) measured in the draining solution when Cd (II) solution was continuously applied to the sorbent. This shows that acid regeneration is sufficient without base treatment. The adsorption is reversible due largely to the cation-proton ion exchange [18].

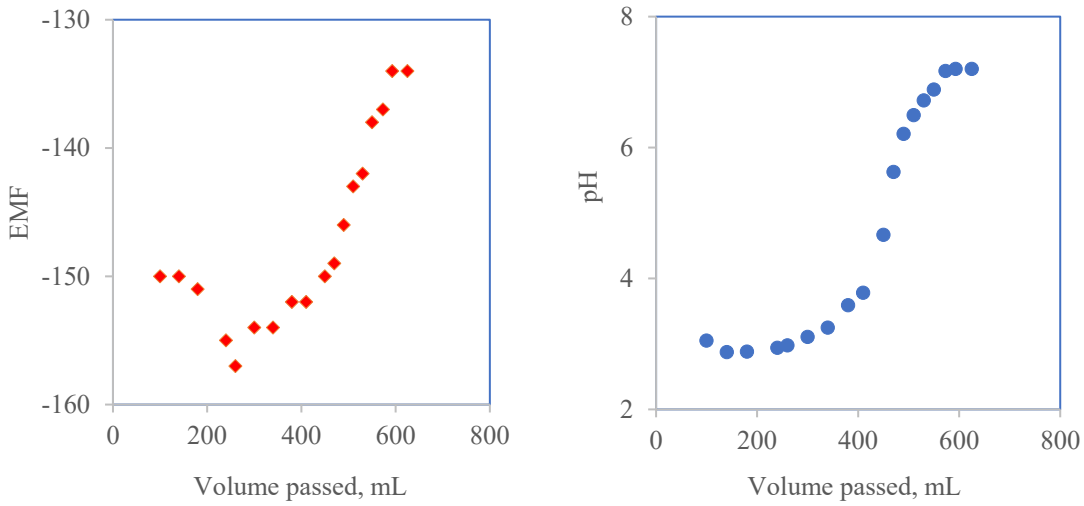

(a) (b)

Figure 18. Column Cd^{2+} adsorption with 200 ppm Cd^{2+} in dilute pH 7.2 Tris-HCl buffer as feeding solution. (a) Cd(II)-ISE potential (b) pH vs. the solution volume collected.

3.5. LEAD ADSORPTION

3.5.1. Time response monitored with Lead ISE

Unlike cadmium solutions, lead precipitates when the pH is above neutral. Thus, all lead adsorption studies were performed in buffered media at a pH below 7. Like cadmium adsorption, there was a gradual reduction in electrode potential when the biosorbent was present in the lead ion solution. Figure 19 (a) shows the electrode potential change in buffered solution with 500 ppm of initial Pb (II) concentration after potato base sorbent was added.

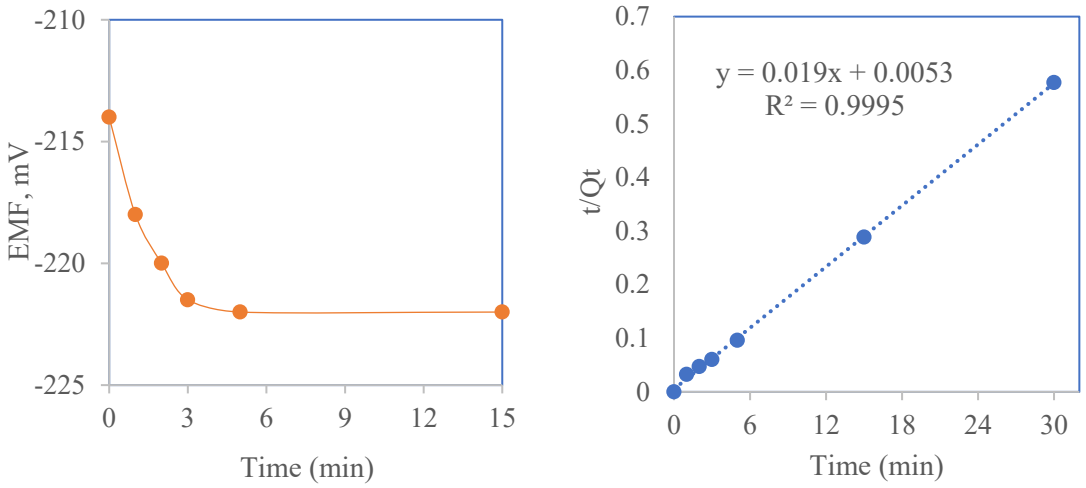

(a) (b)

Figure 19. (a) Time response of the lead (II) electrode with 40 mL of 500 ppm initial lead concentration in acetic acid buffer of pH 5.6 when 0.20 g of base treated potato peel was added. (b) Linear plot of the second order model.

Figure 19 (b) shows a second order kinetics graph with excellent fitting, suggesting that the adsorption of lead also has a great deal of chemisorption. In addition, the FTIR spectrum also shows a reduction of the carbonyl stretch peak with pumpkin

peels. This confirms that the cadmium (II) and lead (II) ions likely involve the C=O bonds in the process of chemisorption.

3.5.2. Lead Adsorption Isotherms

Adsorption isotherms were also produced with various initial Pb (II) concentrations, and the equilibrium concentrations were measured with the lead (II) electrode and ICP-OES. Similar to Cd (II) ion adsorption, the isotherm curves for lead adsorption all showed an L-shape and fit well with the Freundlich model. Figure 20 shows the lead adsorption isotherm and Freundlich fitting using potato sorbent.

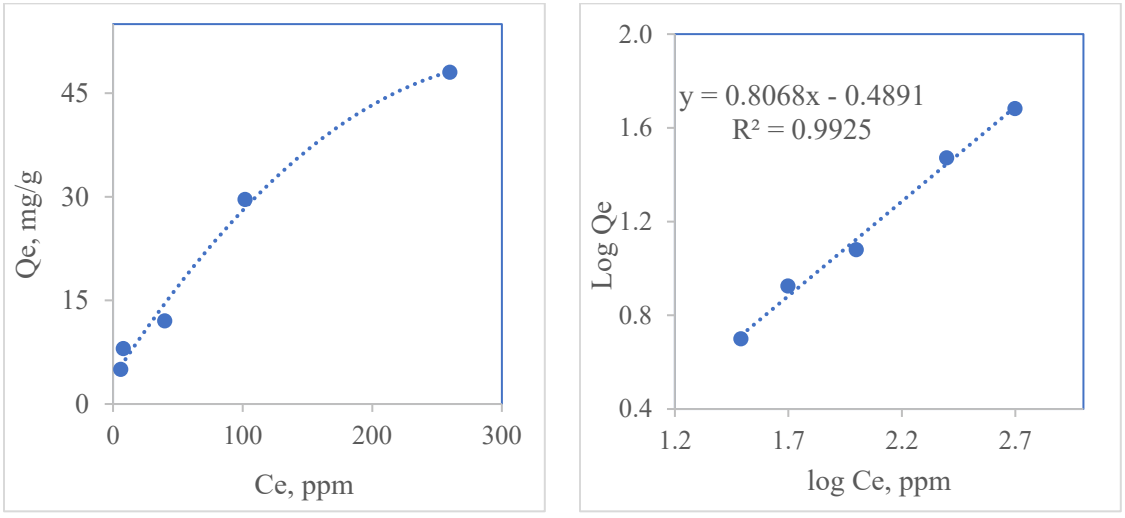

(a) (b)

Figure 20. (a) Adsorption isotherm and (b) Freundlich fitting equations for Pb (II) adsorption on base treated potato biosorbents.

Table 4 summarizes the kinetic and isotherm studies for lead (II) ion adsorption of the biowaste sorbents at pH 5.6. Comparing tables 2 and 3 at a pH of 5.6, the biowaste sorbent adsorption to both ions are comparable in K_f and n values at the same solution

pH. The kinetic parameter obtained Q_e, k_2 values were lower at a lower concentration. Table 3 also shows that the Q_e values derived from equilibrium measured concentration and from the second order kinetic plots are very close, confirming the adsorption follows the second order. For the equilibrium concentration sets that were run with ICP-OES, the Q_e values are close and more often lower than the ISE measured values. This difference may be because the lead-selective electrode drifts towards lower electrode potentials gradually along the adsorption process, which will contribute negative error (lower concentration) in the calculated C_e values.

Table 4. Freundlich isotherm fitting and kinetics constants for Pb (II) ion at various sorbents measured with Pb (II)-ISE and ICP at a pH of 5.6 with 250 ppm initial Pb (II) concentration.

Sorbent	K_f	n	Q_e^m -ISE, ICP*	$Q_e^{cal\#}$	K_2	R^2
Pumpkin base	2.5	1.6	36,28	37	0.023	0.999
Potato base	4.5	1.9	42,30	44	0.012	0.999

*: Q_e^m-ISE, ICP are the values obtained in mg/g with the equilibrium concentration of C_0 ppm initial concentration measured with ISE and ICP, respectively.

: Q_e^{cal} is the value derived in mg/g from the second order kinetic plot of the same initial concentration.

Although the Q_e^m values for both the ICP and ISE methods show adsorption of lead ions with both biosorbents, there is a larger discrepancy compared to the cadmium adsorption study. This is largely due to an electrode drift after prolonged use using the Pb (II)-ISE. However, the Q_e^m value obtained from ICP still shows a significant amount of adsorption of lead ions.

There may be multiple mechanisms undergoing the adsorption process between the biosorbent peels and the metal ions. One possible mechanism that is confirmed by these studies is through the involvement of carboxylic acid functional groups. The base treatment of the sorbents may serve to deprotonate the carboxylic acid and allow for either lead or cadmium ions to complex with the negatively charged oxygen groups. It is probable that a combination of both mechanisms shown in figure 21 are involved in the adsorption process.

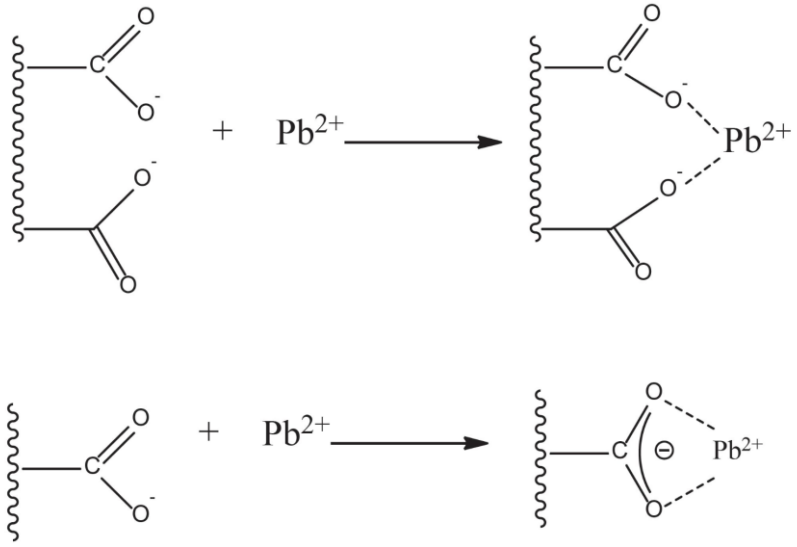

Figure 21. Adsorption mechanism of carboxylic acid groups containing adsorbent polymer for lead ion. [71]

CHAPTER 4:

CONCLUSION

This study shows that simple ion selective electrodes of metals can be used to in-situ continuously monitor the adsorption process of heavy metals onto solid substrates. Biowaste sorbents such as pumpkin and potato peels can efficiently adsorb toxic cations cadmium and lead from aqueous solutions. With base treated sorbents, the sorbents give higher adsorption specifically at high pH which could be accounted for favorable chemisorption when the surface is less positively or even negatively charged. The sorbent can also be regenerated with acid washing. The ISE measurements gave comparable equilibrium concentrations compared to ICP-OES measurements. Ion-selective electrodes do not need sample pretreatment especially in buffered medium and is a much faster method to follow the kinetic process. Other ion-selective electrodes can be applied to similar studies. However, it must be noted that the lead-selective electrode showed major drifts in the measured potential when no change in the lead concentration was occurring possibly due to interfering ions. This led to higher Q_e values for the lead ion compared to the ICP-OES value.

The ease of using ion selective electrodes allows for more experiments to be done in a less complex and cheaper method to analyze many other biowaste sorbents in their effectiveness to adsorb toxic heavy metals from drinking water. Kinetic studies also offer a major advantage in understanding the adsorption process in a molecular level and allows for further advancement in the field of environmental studies.

REFERENCES

1- Chowdhury, S., Mazumder, J.M.A., Al-Attas, O. and Husain, T. (2016) Heavy Metals in Drinking Water: Occurrences, Implications, and Future Needs in Developing Countries, *Science of The Total Environment*. **569-570**, 476-488.

2- Huff, J., Lunn, R.N., Waalkes, M.P., Tomatis, L. and Infante, P.F. (2007) Cadmium-induced Cancers in Animals and in Humans. *Int J Occup Environ Health*. 13(2), 202-212.

3- Kubier, A., Wilkin, R.T. and Pichler, T. (2019) Cadmium in Soils and Groundwater: A review. *Appl Geochem.* 108, 1-16.

4- National Center for Environmental Health, Division of Environmental Health Science and Practice. *Lead in Drinking Water*. CDC, last revised: Feb 2023. https://www.cdc.gov/nceh/lead/prevention/sources/water.htm#print

5- Zhang, R., Wilson, V.L., Hou, A., Meng, G. (2015) Sources of Lead Pollution, Its Influence on Public Health and The Countermeasures, Int J of Health Animal Science & Food Safety. 2 (1), 18-31.

6- Payne, M. (2008) Lead in Drinking Water. *Canadian Medical Association Journal*. 179 (3), 253-254.

7- Pragst, F., Stieglitz, K., Runge, H., Runow, K., Quig, D., Osborne, R., Runge, C., Ariki, J. (2017) High Concentrations of Lead and Barium in Hair of the Rural Population Caused by Water Pollution in the Thar Jath Oilfields in South Sudan. *Forensic Science International*. 274, 99-106.

8- Rahimzadeh, M.R., Kazemi, S. and Moghadamnia, A. A. (2017) Cadmium toxicity and treatment: An update. *Caspian J Intern Med.* **7**(3), 135–145.

9- Salim, R., Al-Subu, M. and Dawod, E. (2008) Efficiency of removal of cadmium from aqueous solutions by plant leaves and the effects of interaction of combinations of leaves on their removal efficiency. *J. Environ. Manage,* **87**, 521–532.

10- Zheng, W., Li, X., Wang, F., Yanga, Q., Dengb, P. and Zenga, G. (2008) Adsorption removal of cadmium and copper from aqueous solution by areca-a food waste. *J. Hazard. Mater,* **157**, 490–495.

11- Tan, G. and Xiao, D. (2009) Adsorption of cadmium ion from aqueous solution by ground wheat stems. *J. Hazard. Mater*, **164**, 1359–1363.

12- Azouaou, N., Sadaouia, Z. and Djaafri, A.; Mokaddem, H. (2010) Adsorption of cadmium from aqueous solution onto untreated coffee grounds: equilibrium kinetics and thermodynamics. *J. Hazard. Mater*. **184**, 126–134.

13- Semerjian, L. (2010) Equilibrium and kinetics of cadmium adsorption from aqueous solutions using untreated Pinus halepensis sawdust. *J. Hazard. Mater*, **173**, 236–242.

14- Ammari, T.G. (2014) Utilization of a natural ecosystem bio-waste; leaves of Arundo donax reed, as a raw material of low-cost eco-biosorbent for cadmium removal from aqueous phase, *Ecological Engineering*, **71**, 466–473.

15- Mathew, B. B., Jaishankar, M., Biju, V. G. and Beeregowda, K. N. Role of Bioadsorbents in Reducing Toxic Metals. *J. of Toxicology* 2016, Article ID 4369604.

16- Carolin C. F. , Kumar P. S., Saravanan A., Joshib G.J. and Naushad M. (2017) Efficient techniques for the removal of toxic heavy metals from aquatic environment: a review. *J Environ Chem Eng*, (5), 2782-2799.

17- Malik, L.A., Bashir, A. and Qureashi, A. (2019) Detection and removal of heavy metal ions: a review. *Environ Chem Lett,* **17***,* 1495-1521.

18- Kwikima, M. M., Marteso, S. and Chebude, Y. (2021) Potentials of agricultural wastes as the ultimate alternative adsorbent for cadmium removal from wastewater. A review. *Scientific Africa*, **13**, e00934.

19- Palabıyıka, B.B., Selcukb, H. and Oktem,Y.A., (2019) Cadmium removal using potato peels as adsorbent: kinetic studies. *Desalination and Water Treatment*, **172**, 148–157.

20- Inoue, K., Parajuli, D., Ghimire, K.N., Biswas, B.K., Kawakita, H., Oshima, T. and Keisuki, O. (2017) Biosorbents for Removing Hazardous Material and Metalloids. *Materials*. **10**(8). 857

21- Sampaio, L.S., Petropoulous, S.A., Alexopoulos, A., Heleno, S.A., Santos-Buelga, C., Barros, L., Ferrera, I.C.F.R. (2020) Potato peels as sources of functional compounds for the food industry. *Trends in Food Science & Technology*, **103**, 118-129.

22- Javed, A., Ahmas, A., Tahir, A., Shabbir, U., Nouman, M., Hameed, A. (2019) Potato peel waste- its nutraceutical, industrial, and biotechnological applications. *AIMS Agriculture and Food,* **4**(3), 807-823.

23- Hussain, A., Kausar, T., Sehar, S., Sarwar, A., Ashraf, A.H., Jamil, M.A., Noreen, S., Rafique, A., Iftikhar, K., Quddoos, M.Y., Aslam, J., Majeed, M.A. (2022) A Comprehensive review of functional ingredients, especially bioactive compounds present in pumpkin peel, flesh and seeds, and their health benefits. *Food Chemistry Advances*, **1**, 100067.

24- Badr, S.E.A., Shaaban, M., Elkholy, Y.M., Helal, M.H., Hamza, A.S., Masoud, M.S., El Safty, M.M. (2010) Chemical composition and biological activity of ripe pumpkin fruits

(*Cucurbita pepo L.)* cultivated in Egyptian habitats. *Natural Product Research*, **25**(16), 1524-1539.

25- Bahramsoltani, R., Farzaei, M. H., Abdolghaffari, A. H., Rahimi, R., Samadi, N., Heidari, M., Esfandyari, M., Baeeri, M., Hassanzadeh, G., Abdollahi, M., Soltani, S., Pourvaziri, A., Amin, G. (2017). Evaluation of phytochemicals, antioxidant and burn wound healing activities of *Cucurbita moschata* Duchesne fruit peel. *Iranian journal of basic medical sciences*, **20**(7), 798–805.

26- Wypych, G. (2018) Mechanisms of Adhesion. *Handbook of Adhesion Promoters* (pp. 5-44), ChemTec Publishing.

27- Ballantine Jr., D.S., Martin, S.J., Ricco, A.J., Frye, G.C., Wohltjen, H., White, R.M., Zellers, E.T. (1997) Materials Chacterization. *Acoustic Wave Sensors Theory, Design, and Physico-Chemical Applications Applications of Modern Acoustics* (pp. 150-221) Academic Press.

28- Webb, P.A. (2003) Introduction to Chemical Adsorption Analytical Techniques and their Applications to Catalysis. *MIC Technical Publications*, 1-12.

29- Deng, F., Luo, X., Ding, L., Luo, S. (2019) Application of Nanomaterials and Nanotechnology in the Reutilization of Metal Ion From Wastewater. *Nanomaterials for the Removal of Pollutants and Resource Reutilization Micro and Nano Technologies* (pp. 149-178), Elsevier.

30- Mathew, B.B., Jaishankar, M., Biju, V.G., Beeregowda, K.N.(2016) Role of Bioadsorbents in Reducing Toxic Metals. *Journal of Toxicology*, vol. **2016**.

31- Deng, F., Luo, X., Ding, L., Luo, S. (2019) Application of Nanotechnology in the Removal of Heavy Metal From Water. *Nanomaterials for the Removal of Pollutants and Resource Reutilization Micro and Nano Technologies* (pp. 83-147), Elsevier.

32- Hammond, K.D., Conner Jr., W.C. (2013) Chapter One - Analysis of Catalyst Surface Structure by Physical Sorption. *Advances in Catalysis*, **56**, 1-101.

33- Kalam, S., Abu-Khamsin, A.S., Kamal, M.S., Patil, S. (2021) Surfactant Adsorption Isotherms: A Review. *ACS Omega*, **6**(48), 32342-32348.

34- Nounou, M.N., Nounou, H.N. (2010) Multiscale estimation of the Freundlich adsorption isotherm. *International Journal of Environmental Science & Technology* **7**, 509–518.

35- DeMessie, J.A., Sorial, G.A., Sahle-DeMessie, E. (2022) Chapter 9 - Removing chromium (VI) from contaminated water using a nano-chitosan–coated diatomaceous earth. *Separation Science and Technology*, **15**, 163-176.

36- Morf, W.E. (1981) *The Principles of Ion-Selective Electrodes and of Membrane Transport*. Elsevier, pp. 1-5.

37- Lakshminarayanaiah, N. (2012) Membrane Electrodes. Elsevier.

38- Pohanka, M., Skládal, P. (2008) Electrochemical Biosensors – Principles and Applications. *Journal of Applied Biomedicine,* **6**(2), 57-64.

39- Heising, J.K., Bartels, P.V., Van Boekel, M.A.J.S., Dekker, M. (2014) Non-destructive sensing of the freshness of packed cod fish using conductivity and pH electrodes. *Journal of Food Engineering*, **124**, 80-85.

40- Cadmium Ion Selective Electrode User Guide. *Thermo Scientific*.

41- Lead Ion Selective Electrode User Guide. *Thermo Scientific*.

42- Tang, X., Wang, P., Buchter, G. (2018) Ion-Selective Electrodes for Detection of Lead (II) in Drinking Water: A Mini-Review. *Environments*, **5**(9), 95.

43- Ensafi, A.A., Meghdadi, S., Sedighi, S. (2009) Sensitive Cadmium Potentiometric Sensor Based on 4-Hydroxy Salophen as a Fast Tool for Water Samples Analysis. *Desalination*, **243**(1-3), 336-345.

44- Piñeros, M.A., Shaff, J.E., Kochian, L.V. (1998). Development, Characterization, and Application of a Cadmium-Selective Microelectrode for the Measurement of Cadmium Fluxes in Roots of Thlaspi Species and Wheat. *Plant physiology*, **116**(4), 1393–1401.

45- Freiser, H. (1980) Ion-Selective Electrodes in Analytical Chemistry. Plenum Press, vol. 2, pp. 208.

46- Li, X., Ma, X., Huang, M. (2009) Lead(II) ion-selective electrode based on polyaminoanthraquinone particles with intrinsic conductivity. *Talanta*, **78**(2), 498-505.

47- Olesik, J.W. (2011) Peer Reviewed: Fundamental Research in ICP-OES and ICPMS. *Analytical Chemistry,* **68**(15), 469A-474A.

48- Wilschefski, S. C., Baxter, M. R. (2019). Inductively Coupled Plasma Mass Spectrometry: Introduction to Analytical Aspects. *The Clinical biochemist. Reviews*, **40**(3), 115–133.

49- Morrison, C., Sun, H., Yao, Y., Loomis, R.A., Buhro, W.E. (2020) Methods for the ICP-OES Analysis of Semiconductor Materials. *Chemistry of Materials*, **32**(5), 1760-1768.

50- Fadlelmoula, A., Pinho, D., Carvalho, V. H., Catarino, S. O., Minas, G. (2022). Fourier Transform Infrared (FTIR) Spectroscopy to Analyse Human Blood over the Last 20 Years: A Review towards Lab-on-a-Chip Devices. *Micromachines*, **13**(2), 187.

51- Wegener, A., Wiesmann, M., Luschas, P., Vogel, K., Pursch, M. (2019) ICP-OES Hyphenation: Speciation and Quantification of Polydimethylsiloxanes at Trace Levels. *Spectroscopy*, **34**(1), 38-46.

52- Wiltsche, H., Wolfgang, M. (2020) Merits of microwave plasmas for optical emission spectrometry – characterization of an axially viewed microwave-sustained, inductively coupled, atmospheric-pressure plasma (MICAP). Journal of Analytical Atomic Spectrometry, 35(10), 2369-2377.

53- Pappas R. S. (2012). Sample Preparation Problem Solving for Inductively Coupled Plasma-Mass Spectrometry with Liquid Introduction Systems I. Solubility, Chelation, and Memory Effects. *Spectroscopy*, **27**(5), 20–31.

54- Optima 2100 DV Instruction Manual. Perkin Elmer.

55- Lin, S.Y., Dence, C.W. (1992) Fourier Transform Infrared Spectroscopy. In Faix, O., *Methods in Lignin Chemistry* (pp. 83-89), Springer Series in Wood Science.

56- Margariti, C. (2019) The application of FTIR microspectroscopy in a non-invasive and non-destructive way to the study and conservation of mineralised excavated textiles. *Heritage Science*, **7**(63).

57- D-glucose Infrared Spectrum. *NIST Chemistry WebBook SRD 69*. Obtained by the Coblenz Society.

58- Azad, M. and Avin, A. (2018) Scanning Electron Microscopy (SEM): A Review. *Proceedings of 2018 International Conference on Hydraulics and Pneumatics*, HERVEX, Baile Govora, Romania, 7-9 November 2018, 1-9.

59- Danilatos, G.D., Robinson, V.N.E. (1979) Principles of Scanning Electron Microscopy at High Specimen Chamber Pressures. *Scanning*, **2**, 72-82.

60- Subramanian, K.S., Janavi, G.J., Marimuthu, S., Kannan, M., Raja, K., Haripriya, S., Sharmila, D.J.S., Moorthy, P.S. (2018) Scanning Electron Microscopy: Principle, Components and Applications. *A Textbook on Fundamentals and Applications of Nanotechnology* (pp. 81-90). Daya Publishing House.

61- Kojuncu, Y., Bundalevska, J.M., Ay, U., Cundeva, K., Stafilov, T. and Akcin, G. (2004) Atomic absorption spectrometry determination of Cd, Cu, Fe, Ni, Pb, Zn, and Tl traces in seawater following flotation separation. *Separation Science and Technology*, **39**, 2751–2765.

62- Cvetkovi, J., Arpadjan, S., Karadjova, I. and Stafilov, T. (2006) Determination of cadmium in wine by electrothermal atomic absorption spectrometry. *Acta Pharmaceutica*, **56**, 69–77.

63- Nedeltcheva, T., Atanassova, M., Dimitrov, J. and Stanislavova, L. (2005) Determination of mobile form contents of Zn, Cd, Pb and Cu in soil extracts by combined stripping voltammetry. *Analytica Chimica Acta*, **528**, 143–146.

64- Gumpu, M. B., Sethuraman, S., Krishnan, U. M. and Rayappan, J. B. B. (2005) A review on detection of heavy metal ions in water – an electrochemical approach. *Sensors and Actuators B: Chemical*, **213**, 515–533.

65- De Marco, R., Clarke, G. and Pejcic, B. (2007) Ion-selective electrode potentiometry in environmental analysis. *Electroanalysis*, **19**, 1987–2001.

66- Ensafi, A.A., Meghdadi, S. and Sedighi, S. (2009) Sensitive cadmium potentiometric sensor based on 4-hydroxy salophen as a fast tool for water samples analysis. *Desalination*, **242**(1–3):336–345. doi:10.1016/j.desal.2008.06.002

67- Gupta, V. K., Ganjali, M. R., Norouzi, P., Khani, H., Nayak, A. and Agarwal, S. (2011) Electrochemical analysis of some toxic metals by ion-selective electrodes. *Critical Reviews in Analytical Chemistry*, **41**, 282–313.

68- Crespo, G.A. (2017) Recent Advances in Ion-selective membrane electrodes for in situ environmental water analysis. *Electrochim. Acta*, **245**, 1023-1034.

69- Masel, R. (2019) Principles of adsorption and reaction on solid surfaces. *Wiley Interscience publications. England*. pp. 235 -248.

70- Miller, J.C., Miller, J.N. (1991) Basic Statistical Methods for Analytical Chemistry. Part 2. Calibration and Regression Methods. A Review. *Analyst,* **116**, 3-14.

71- Hosseinzadeh, M. (2019) Sorption of Lead Ions form Aqueous Solutions by Carboxylic Acid Groups Containing Adsorbent Polymer. *Journal of the Chilean Chemical Society*, **64**(2).

Vita

Name:	*Taha Fadlou Allah*
Baccalaureate Degree:	*Bachelor of Science, St. John's University, Queens,* *Major: Chemistry*
Date Graduated:	*May 2021*